

Review

Review of Particle Filters for Internal Combustion Engines

Rui Dong ¹, Zhiqing Zhang ¹ , Yanshuai Ye ^{1,*} , Huiqiong Huang ¹ and Chao Cao ²

¹ School of Mechanical and Automotive Engineering, Guangxi University of Science and Technology, Liuzhou 545006, China; 221068187@stdmail.gxust.edu.cn (R.D.); zhangzhiqing@gxust.edu.cn (Z.Z.); huiqiongh@gxust.edu.cn (H.H.)

² Shanghai Wenze Communication Technology Center, Shanghai 201712, China; shwztx@yeah.net

* Correspondence: yeyanshuai@gxust.edu.cn

Abstract: Diesel engines have gradually become one of the main forces in the human transportation industry because of their high efficiency, good durability, and stable operation. However, compared with gasoline vehicles, the high emission of diesel vehicles forces manufacturers to introduce new pollutant control technologies. Although the particulate matter emissions of gasoline vehicles are lower than that of diesel vehicles, with the popularity of gasoline vehicles and the continuous rise of power, the impact of these particles on the environment cannot be ignored. Therefore, diesel particulate filters and gasoline particulate filters have been invented to collect the fine particles in the exhaust gas to protect the environment and meet increasingly stringent emission regulations. This paper summarizes the research progress on diesel particulate filters and gasoline particulate filters at present and comprehensively introduces the diesel particulate filter and gasoline particulate filter from the mechanism, composition, and operation processes. Additionally, the laws and regulations of various countries and the impact of gas waste particulates on the human body are described. In addition, the mechanisms of the diesel particulate filter, gasoline particulate filter, and regeneration were studied. Finally, the prospects and future directions for the development of particle filters for internal combustion engines are presented.

Keywords: diesel particulate filter; gasoline particulate filter; regeneration; pressure drop; deposition



Citation: Dong, R.; Zhang, Z.; Ye, Y.; Huang, H.; Cao, C. Review of Particle Filters for Internal Combustion Engines. *Processes* **2022**, *10*, 993. <https://doi.org/10.3390/pr10050993>

Academic Editor: Zhihua Wang

Received: 23 March 2022

Accepted: 12 May 2022

Published: 17 May 2022

Publisher's Note: MDPI stays neutral with regard to jurisdictional claims in published maps and institutional affiliations.



Copyright: © 2022 by the authors. Licensee MDPI, Basel, Switzerland. This article is an open access article distributed under the terms and conditions of the Creative Commons Attribution (CC BY) license (<https://creativecommons.org/licenses/by/4.0/>).

1. Introduction

1.1. Research Background

The good fuel economy, reliability, and durability of diesel vehicles [1] makes them the main power source of medium and heavy vehicles [2,3]. However, the high emissions of diesel engines limit their applications. The exhaust gas of diesel engines contains particulate matter (PM), carbon monoxide (CO), hydrocarbons (HC), and nitrogen oxides (NO_x) [4]. PM from diesel engines [5,6] has a serious impact on human health, leading to a sharp increase in cardiovascular and respiratory diseases in particular [7]. PM are easily inhaled in the bronchi and deep alveoli of the respiratory tract, causing people to suffer from various respiratory diseases as a result. There has also been evidence in recent years that PM can damage human neurodevelopment [8] and cognitive function [9]. In fact, PM was classified as a carcinogen in 2012 by the World Health Organization (WHO) [10].

In order to deal with people's health problems and prominent environmental problems, governments are constantly tightening the control of PM emissions from diesel vehicles. China has issued new limits and measurement methods for emissions from light-duty vehicles (China VI). Compared with the old standard, the new standard reduces PM emissions and brings the number of particles into the regulatory scope. The same situation has occurred in Europe, the United States, and most countries around the world [11].

Therefore, it is necessary to develop an effective way to reduce PM emissions and comply with the increasingly stringent emission regulations [12,13]. According to the current research, there are many methods to control PM emission, such as blended fuel [14,15],

biodiesel [16,17], the improvement of engine structure [18], and so on. However, the most effective way to control PM is a particulate filter [19]. This article focuses on the basic conditions of a particulate filter [20].

1.2. Present Situation of Diesel Particulate Filter

The pollution emissions from diesel engines limit the further application of diesel engines [21–23]. Controlling diesel engine exhaust emissions has always been important work to meet the increasingly stringent regulations and the need for environmental protection. At present, there are many methods to control the PM emissions of diesel engines, such as engine type [24], after-treatment system [25], working point [26], and fuel and oil type [27]. Among them, the DPF is the most representative technical method. Based on the mechanism of particle deposition in DPFs, DPFs can reduce more than 90% of diesel particles (including soot, soluble organic matter (SOF), sulfate, and ash) [28].

DPFs have been studied for over 30 years. In previous experiments, most DPFs could reduce the HC emissions by 85%–95% and carbon monoxide by 50%–90%. Therefore, DPFs are considered a feasible diesel engine after-treatment method to meet the increasingly stringent PM requirements.

At present, although DPF technology is an effective way to control particulate matter emissions and meets the current and future emission regulations, it is still in the optimization and cost reduction stage [29]. The filtration efficiency of a DPF is usually higher than 95%, and the particulate matter emission of a diesel engine equipped with a DPF system is one order of magnitude lower than the current laboratory certification limit ($6.0 \times 10^{11} \# / (\text{kW} \cdot \text{h})$) [30].

2. Diesel Particulate Matter

2.1. Composition of Diesel Particulate Matter

PM emitted by diesel engines is a very complex mixture. It is produced by a series of physical and chemical reactions between the gaseous, liquid, and solid substances in the exhaust pipe and the post-treatment catalyst at the exhaust stroke; soot is produced by the high temperature and anoxic environment during the combustion of fuel oil.

In general, the main components of PM include dry soot, SOF, and sulfate [31]. When the diesel fuel is mixed unevenly in the combustion chamber and there is a local concentration area, it will lead to the local anoxic combustion of the diesel fuel mixture. Dry soot is easily produced when the exhaust temperature is high. Soluble organic fractions account for the majority of PM emitted by diesel and are composed of unburned and fully burned components of a fuel and lubricating oil [32]. When the exhaust temperature is low, it is adsorbed on the surface of various organic fractions and discharged along with the exhaust. These organic components include various unburned organic compounds, oxygenated organic compounds, hydrocarbons, and other derivatives. Sulfates are produced by the presence of sulfur in diesel fuel. Figure 1 shows the specific composition of PM.

The particles produced by the engine are generally divided into five categories according to their particle diameter: (1) large particles $>10 \mu\text{m}$, (2) coarse particles $2.5\text{--}10 \mu\text{m}$ (PM_{10}), (3) fine particles $0.1\text{--}2.5 \mu\text{m}$ ($\text{PM}_{2.5}$), (4) ultra-fine particles $50\text{--}100 \text{ nm}$ ($0.1 \mu\text{m}$) ($\text{PM}_{0.1}$), and (5) nanoparticles $<50 \text{ nm}$. It can be seen that the diameter of particles emitted by the direct injection engine is within $2.5 \mu\text{m}$ and the $\text{PM}_{2.5}$ index includes these particles. Figure 2a shows that the distribution of particle diameter in the exhaust gas is logarithmic under the normal operation of the engine. It can be observed that most particle sizes are concentrated in $50\text{--}100 \text{ nm}$ sizes. Figure 2b shows the mass distribution of particles. Compared with the particle size, the mass distribution shows a more concentrated state. The particle mass is concentrated near 100 nm .

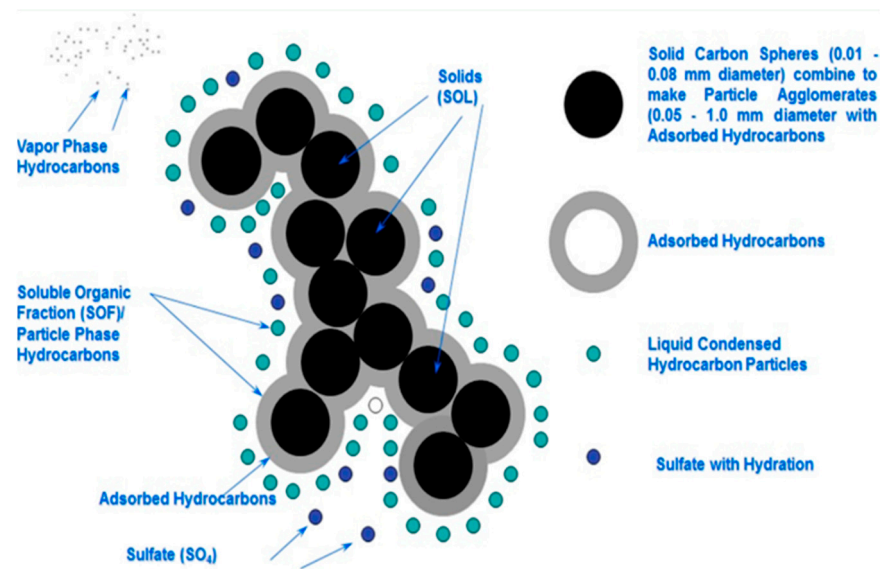


Figure 1. The specific composition of PM [33].

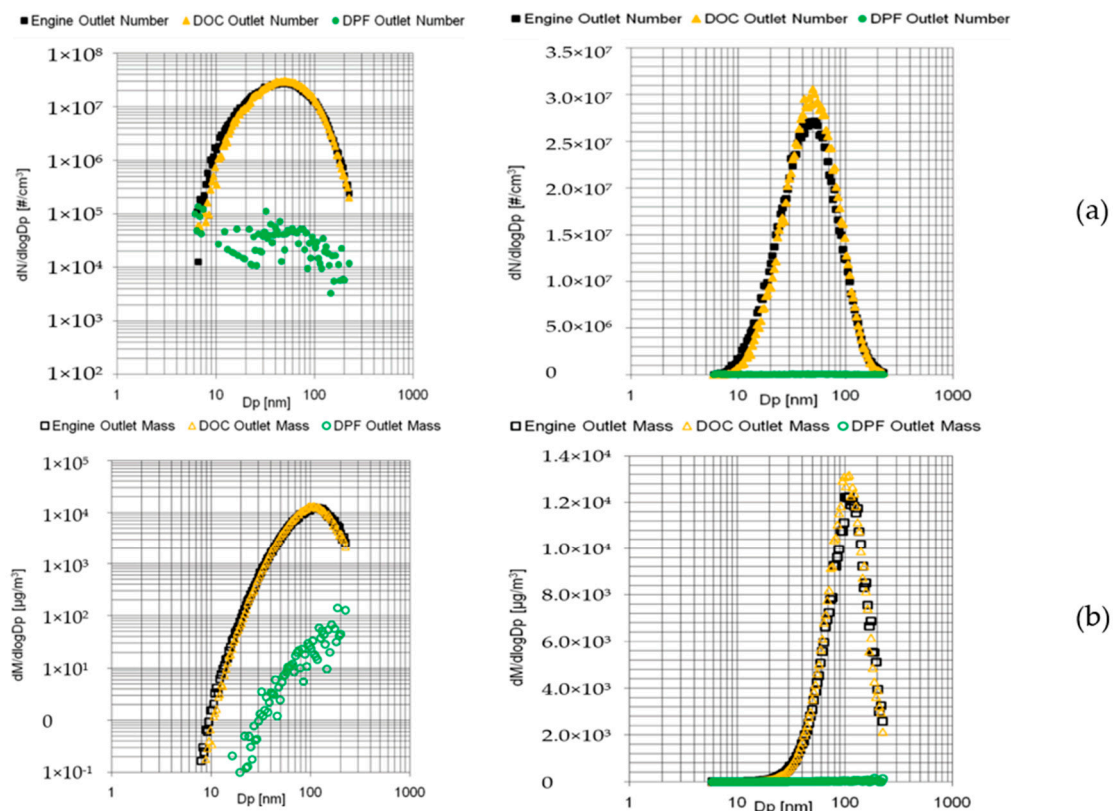


Figure 2. Mass-size distribution of PM (a) and the number of particles (b) under normal engine operation (1750 RPM/3.5 bar BMEP) [34].

2.2. Harm of Particulate Matter

Meteorologists and medical experts believe that the fine particle matter-like haze can influence human health in a variety of ways, other than dust storms, it is recognized as an important risk factor for many chronic diseases, including cardiovascular disease [35]. The combustion of fossil fuels is a major source of fine particulates, although they are controlled by pre-treatment or post-treatment [36].

Particles with a diameter between 2.5 and 10 μm can enter the upper respiratory tract and some of them can be discharged from the body through the sputum. In addition, they will be blocked by the villi inside the nasal cavity, and are thus relatively less harmful to human health. However, fine particles with a diameter of less than 2.5 μm , which is one-tenth of the size of human hair, are not easily blocked. It is reported that the smaller particles are the most harmful to human health [8].

The physiological structure of the human body determines that we have no ability to filter and block PM_{2.5}. When inhaled into the human body, these fine particles will directly enter the bronchi, interfere with the gas exchange in the lungs, and cause diseases such as asthma [37], bronchitis [38], and cardiovascular diseases [39].

Each person inhales about 10,000 L of air on average every day. The dust entering the alveoli can be absorbed rapidly, and directly enter the blood circulation and distribute to the whole body without detoxification by the liver. Secondly, it can damage the ability of hemoglobin to deliver oxygen and compromise blood, which may have serious consequences for patients with anemia and blood circulation disorders. For example, it may aggravate respiratory system diseases and even cause heart diseases such as congestive heart failure and coronary artery disease. In short, these particles can also enter the blood through the bronchi and alveoli, in which harmful gases, heavy metals, etc. are dissolved in the blood, causing greater harm to human health [40].

An epidemiological investigation found that polycyclic aromatic hydrocarbons (PAHs) in urban air particles were related to the incidence and mortality of lung cancer. Fine particles act as carriers in the process of PAHs entering the human body. Most PAHs are adsorbed on the surface of particles, especially the particles with diameters less than 5 μm . In contrast, there are few PAHs on large particles, that is to say, the more PM_{2.5} in the air, the more opportunities we have for exposure to carcinogenic PAHs [41].

Secondly, pregnant women living in an environment full of PM_{2.5} for a long time can experience affected fetal development and defects. In Wuhan, researchers found that excessive PM increased the risk of fetal distress, which was more obvious in winter [42].

In EU countries, PM_{2.5} leads to an 8.6-month reduction in life expectancy. In China in Asia, despite the high-intensity governance of the government, more than 88% of people are still exposed to excessive PM_{2.5}. It has seriously damaged the health of residents [43]. PM_{2.5} can also be used as a carrier of viruses and bacteria which can promote the spread of respiratory infectious diseases. At present, PM_{2.5} is listed as the air quality standard by the major developed countries in the world, as well as China, Japan, Thailand, and India in Asia.

2.3. Factors Affecting Particulate Matter Generation

There are many factors that affect the generation of particles, such as the design of the engine, the operating conditions, the types of fuel and oil used, etc. All of these will affect the composition of particles.

Considering dry soot in the design of the engine, the trade-off between soot and NO_x can be observed under post-injection conditions. Compared with other emissions, soot emissions are not sensitive to post-injection timing, except for post-injection timing at 20 °CA [44]. Figure 3 shows the changes of particle number and size distribution with different injection volumes after fuel injection amounts post-injection. The soot emission is not sensitive to the injection timing when the injection quantity is small and at 20 °CA, the soot emission increases because of the increase in post-injection fuel. At 40 °CA, the soot is oxidized by the post-injection combustion in the main injection combustion as the post-injection reduces the soot emission.

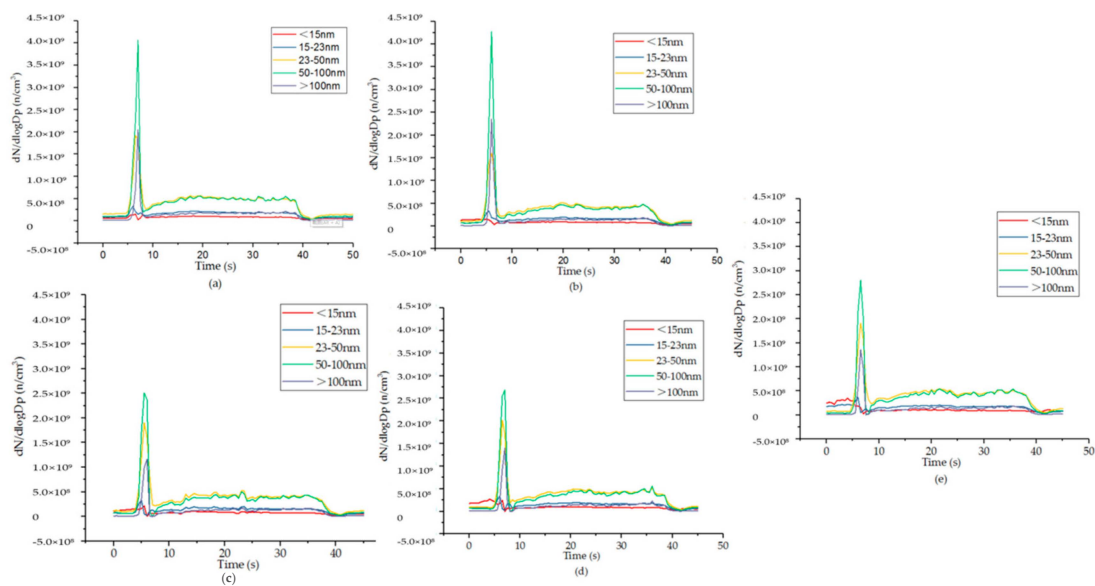


Figure 3. Effects of different amounts of post-injection on PM number size distribution vs. Time: (a) Original; (b) 1 mg; (c) 2 mg; (d) 3 mg; and (e) 4 mg [45].

Fuel characteristics also significantly affect PM and PN emissions and size distribution for Euro VI (without DPF) vehicles [46]. For example, at the beginning of the DPF loading process, the filtration efficiency of particles using biodiesel is 10% lower than that of diesel, but this difference will decrease as the DPF filter is fully loaded [47].

Using optimization methods to optimize the operating conditions of biodiesel and diesel blends to reduce PM emission is also one of the recent research directions. For example, Vellaiyan et al. [48] used the multi-response optimization method to improve the engine performance and emission level by adjusting the concentration of ZnO nanoparticles. Kim et al. [49] studied the emission characteristics of the compression ignition engine using diesel, water, and n-butanol. After changing the water content or n-butanol content, the quality and quantity of engine PM decreased significantly. The binary mixture of diesel and other organic mixtures is also a good way to change the emission of soot particles. For example, Ge et al. experimented with a mixture of diesel and ethanol and found a 46.88% reduction in soot emissions [50].

3. Working Principle of Diesel Particulate Filter

3.1. Structure of Diesel Particulate Filter

At present, most DPFs use the wall-flow honeycomb monolith structure [51] which proves to have a relatively high filtration efficiency, low fuel penalty, and low cost [10]. The filter substrate is composed of thousands of parallel channels with square sides. The passageways are separated by permeable ceramics. For every two adjacent passageways, one is blocked at the entrance and the other is blocked at the exit. When exhaust gas flows through the walls, which are usually made of silicon carbide (SiC), the particles in exhaust gas are deposited on the wall of the inlet passage. As the particulate trap catches increasing amounts of particles, the porosity and permeability of the wall become lower and lower. This process will last a few minutes and is usually called ‘deep-bed’ filtration [10,51]. The purification mechanism changes into deep filter bed filtration. In the process of deep filter bed filtration, the filtration efficiency depends largely on the size, shape, and porosity of micropores. Seungmok et al. [52] compared DPFs with different porosities and found that high porosity is conducive to DPF filtration and reduces the pressure drop in the process. When the soot particles accumulate to a certain thickness, a PM layer will form on the microporous surface of the catcher, and it can be called a “soot cake”. This will greatly enhance the purification efficiency of the particulate trap. However, according to

the research of Fang et al. [53], excessive ash accumulation will lead to the decline of DPF filtration efficiency. When the ash content is greater than 40 g/L, the filtration efficiency decreases gradually with the increase in ash content and the exhaust back pressure will increase, so the particulate trap needs to be replaced or regenerated.

3.2. Particulate Matter Collection Mechanism

The DPF wall should be designed with the optimum porosity so that the exhaust gas can pass through without too much obstruction [54]. The micropores of the particulate trap are usually on the micron scale, the micropores cannot directly play a role in purification as the soot particles are much larger, therefore it is collecting particles through other mechanisms. At present, various mechanisms of particulate collection have been extensively studied, such as the traditional mechanisms of filtration or deposition of suspended particles, including Brownian diffusion, interception, inertial collision, gravity settling, electrostatic attraction, and thermophoretic interdiction [55]. Recently, a DPF load forecasting model based on the capture mechanism and equivalent permeability was proposed by Wang et al. [56]. The average error between the model and the experimental value was 2.72%, which provides a more mathematical reference for filtering and active regeneration strategy.

Whether a DPF meets a successful design standard depends on its capture performance and regeneration performance [57]. Whether the capture performance is good or not mainly depends on whether it has high filtration efficiency, low pressure drop, solid structure, and low escape rate. A good regeneration performance is reflected in the regeneration time, regeneration efficiency, thermal durability, and reliability, as well as whether it has the ability to resist a large number of high-temperature pulsations in the regeneration process in its life cycle [58].

The DPF substrate is a very important part of the particle catcher. The quality of it directly affects the performance and reliability of the filter. DPF materials need to have strong thermal shock resistance, good thermal stability, good mechanical strength, and other properties as the DPF works in the hot end of an exhaust system, which is generally in a complex environment of high temperature and corrosion for a long time. At present, Cordierite ($\text{Cd}_2\text{MgO} \cdot 2\text{Al}_2\text{O}_3 \cdot 5\text{SiO}_2$), SiC, Acicular Mullite (ACM, Al_2SiO_5), Aluminum Titanate (AT, Al_2TiO_5), and Alloy Foam (AF), as shown in Figure 4, are widely used as particle filter materials [29]. The most commonly used filter materials are Cordierite and Silicon Carbide.

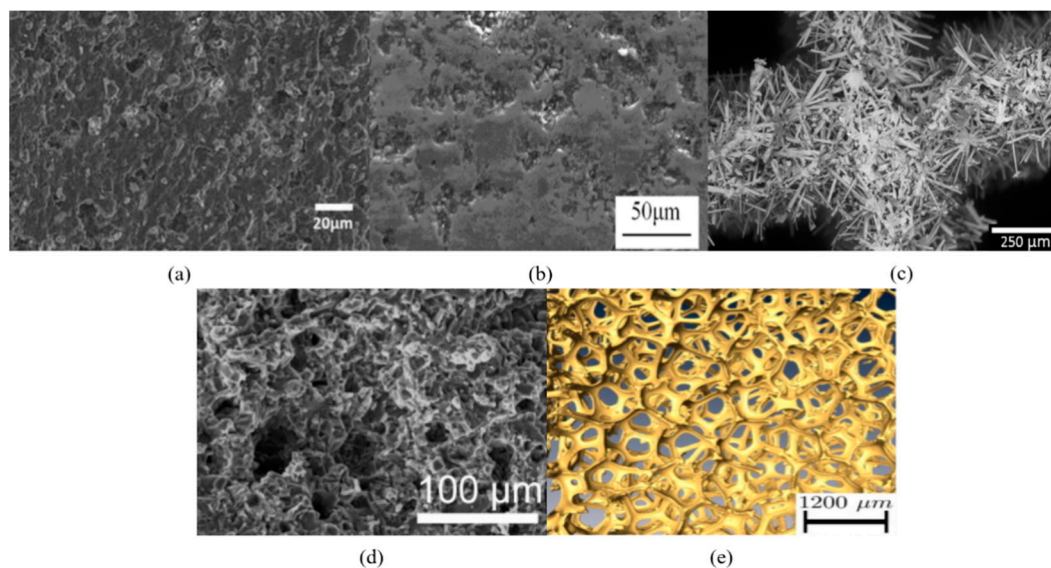


Figure 4. SEM images of the DPF substrate materials: (a) cordierite [59]; (b) SiC [60]; (c) acicular mullite [61]; (d) aluminum titanate [62]; and (e) alloy foam [63].

Cordierite is the most widely used DPF filter material. Its main advantages are low cost, low coefficient of thermal expansion, high temperature resistance [64], and high mechanical strength [65]. Cordierite has a low thermal quality and good coating performance, so its catalyst has a short ignition time [66,67]. The cordierite trap has high conversion efficiencies of CO and HC at low temperatures which can reduce the particles generated in the cold start-up stage and the catalyst heating stage. Cordierite also has some disadvantages, such as poor corrosion resistance, higher radial expansion coefficient than axial expansion coefficient, smaller thermal conductivity, and so on. The internal heat cannot be dissipated, and the filter will crack if the thermal conductivity is low. At the same time, the specific heat capacity of cordierite is smaller, so it is necessary to design a larger wall thickness and channel density, which will lead to an increase in exhaust back pressure and total heat capacity [68]. Therefore, Ki et al. [69] proposed that the sintering atmosphere is an important parameter to measure cordierite. In their study, it was found that the sintering atmosphere affected the pore size and distribution of the DPF and greatly affected its filtration efficiency.

Compared with cordierite, SiC has better heat resistance, heat conduction, and corrosion resistance as well as higher mechanical strength [70]. The thermal conductivity and thermal quality of SiC are very high. During regeneration, it can quickly dissipate the heat generated by PM combustion, reduce the damage to materials, and work in a worse regeneration environment. The main defect of SiC is poor thermal shock resistance, as the filter cracks easily at a high temperature [71]. Therefore, the DPF with SiC as the filter material generally uses ceramic fiber to bond the components into a whole rather than a honeycomb structure. This structure can improve the thermal shock resistance, but also increase the exhaust back pressure. Compared with diesel, SiC-CDPF can help biodiesel reduce power loss [72].

The development of the DPF design includes the optimization of cell shape and cell wall porosity to minimize back pressure on the engine, extend filter service intervals, and promote catalyst coating. Zhang et al. [73] analyzed the structure and operation factors of DPFs by using the orthogonal experimental method. It was concluded that wall thickness and porosity are the two most important factors affecting plugging, which puts forward a scientific basis for improving the DPF structure. Figure 5 shows the loading structure of most DPF experiments.

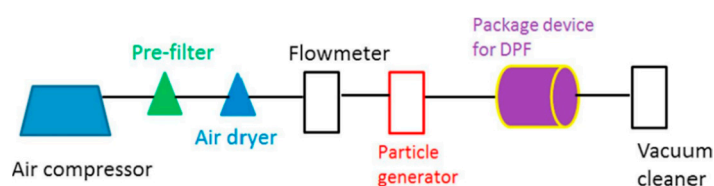


Figure 5. Schematic of the DPF loading system [74].

3.3. Several Types of Diesel Particulate Filter

At present, according to different operation modes, DPFs can be divided into wall-flow DPFs and rotary DPFs.

(1) Wall-flow diesel particulate filters:

Since the muffler was replaced by a diesel particulate trap in the early days, the wall-flow diesel particulate trap has been considered the most common and effective method to remove the particles in diesel engine combustion emissions [75]. The wall-flow honeycomb structure DPF that meets the emission regulations is usually composed of a large number of axial parallel holes [76]. The size of the intercepted particles is directly related to the pore size. The smaller the pore size, the better the interception effect [77]. However, too small a pore size will affect the filtration efficiency [78], so the general pore size is 10–30 μm . One of the two ends is blocked in the filtering channels. The exhaust gas flows through one of the walls and flows out from the other so that the particulate matter can be deposited on the

filter wall surface [79]. The DPF carrier is usually a wall-flow channel structure, as shown in Figure 6. Materials of the filter substrate are mainly cordierite or silicon carbide [80]. The particles are separated from the exhaust gas to the carrier wall by inertia collision, interception, molecular diffusion, gravity sedimentation, and other mechanisms [81]. Wall-flow DPFs are very effective in removing carbon and metal particles, including fine particles with diameters less than 100 nm [82]. Under various operating conditions of the engine, its mass efficiency is more than 95% and its quantity efficiency is more than 99% [83,84]. It also has good mechanical and thermal durability. At the same time, because too much soot cake accumulation will reduce the filtration efficiency, the DPF needs to be regenerated regularly [85]. This requires the DPF to have good thermal and mechanical durability [86].

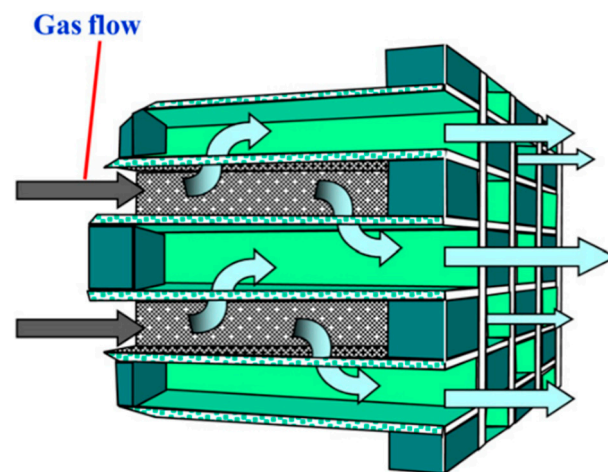


Figure 6. Structure schematic diagram of wall-flow diesel particle filter [87].

(2) Catalytic diesel particulate filters:

Considering that the thermal stress generated by high temperatures during wall-flow DPF regeneration will affect driving safety and service life [88], a method that can regenerate anytime and anywhere, such as passive regeneration and catalytic diesel particulate filters (CDPF), and the corresponding machine, are proposed [29]. The temperature must be above 550 °C during wall-flow DPF regeneration [89], however, the connected exhaust gas cannot reach this temperature, requiring the mixing of catalyst powder into the fuel to make the discharged exhaust gas easier to oxidize [90]. The structure of CDPF is the same as that of wall-flow DPF, but it can prolong the interval time of the DPF active regeneration and service life. The original CDPF, sample slice, and carrier device are shown in Figure 7.



Figure 7. The original CDPF, sample slice, and carrier device [91].

(3) Rotary diesel particulate filters:

Microwave heating is a method of DPF regeneration [92]. Recently, a rotary DPF has received extensive attention. The schematic diagram of the rotary microwave regeneration filter with a silicon carbide foam ceramic filter is shown in Figure 8. The structure of the MR-DPF can be divided into the intake pipe, expansion pipe, filter, contraction pipe, and exhaust pipe. The silicon carbide foam ceramic filter (pore density 50 ppi, length 135 mm, outer diameter 200 mm, inner diameter 80 mm) can be divided into several blocks. In the working process of the rotary MR fluid filter, when the exhaust back pressure reaches a certain value, the filter rotates at a certain angle α (α is the circumferential angle of each filter unit) and starts the microwave generator. In the regeneration stage, one filter unit is heated by microwave, and the other filter unit captures smoke and dust to realize continuous recycling [93]. Experiments show that the catalyst can also be used in a rotating DPF. Using Pd and Pt catalysts on a rotating DPF can reduce the soot reaction temperature and activity [94].

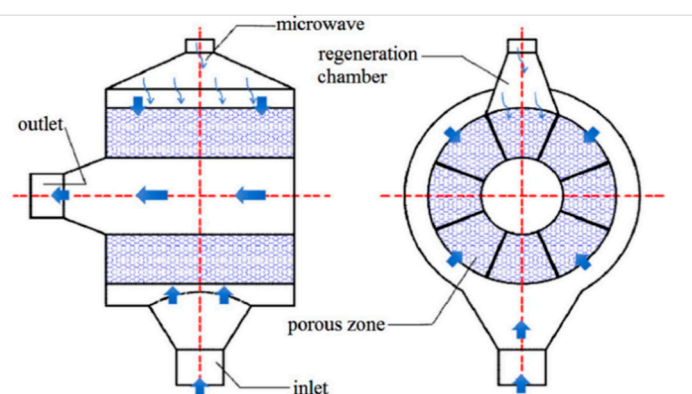


Figure 8. Schematic diagram of a rotary DPF [95].

4. Comparison of Different Regeneration Methods

In the wall-flow DPF, when the exhaust gas flows in from one filter channel and then flows out from the adjacent channel through the porous wall, the particles are effectively trapped on the carrier. The DPF can effectively filter PM from diesel engine exhaust. However, when the particles accumulate in the carrier, the exhaust resistance and exhaust

back pressure of the diesel engine increase, which seriously affects the performance power and economy of the diesel engine [52]. Therefore, it is necessary to choose the right time and effective method to remove the accumulated particles in the DPF carrier. This process is soot regeneration [96]. At present, the biggest challenge for the particulate trap is the regeneration technology.

In the regeneration process, the solid particles collected by the filter body are oxidized by O_2 and NO_2 to form gaseous products dominated by CO_2 [97]. The most important parameter affecting the regeneration performance of the particulate filter is the exhaust gas temperature [98]. However, the active regeneration will be completed when the exhaust temperature reaches more than $550\text{ }^\circ\text{C}$ [99], but the actual exhaust temperature can only reach $200\text{ }^\circ\text{C}$ – $350\text{ }^\circ\text{C}$ [100], and the soot is deposited in the DPF cannot be removed only by the exhaust temperature. There are two solutions proposed: one is active regeneration. The temperature of exhaust gas is increased by other means. When the temperature reaches the point required for carbon smoke oxidation, regeneration will occur. Another one is passive regeneration. The catalytic action of the catalyst is used to reduce the activation energy of particles and reduce the oxidation temperature of soot.

Both regeneration processes are related to the following factors: total accumulated particles [51], particle storage density and distribution [101], exhaust flow rate [102], external heat transfer of the trap [103], and activation reaction capacity of particle matters [104]. The regeneration of particulate filters can be divided into active regeneration and passive regeneration. The two methods can turn the particles collected by the DPF into gas and discharge them so as to achieve the purpose of DPF regeneration.

4.1. Active Regeneration

Under the condition of normal driving or parking, the scheduling conditions cannot meet the requirements of soot oxidation. Therefore, the regeneration must be completed by using the regeneration method with an additional energy supply [105]. Unlike passive regeneration, active regeneration does not need to rely on the duty cycle and exhaust temperature of the engine, and regeneration can be started at any time [106]. In the process of regeneration, the reaction between O_2 and PM mainly depends on increasing the temperature. Tighe et al. characterized the reactions involved in O_2 [107]:



where $C(-)$ is the active site and $C(O)$ is the oxygen-containing functional group. After O_2 participates in the reaction, PM is converted into CO and CO_2 and discharged together with the exhaust gas. For active regeneration, there are many methods. The common ones are post-injection, oil combustion, or electric heater. However, no matter which regeneration method is used, it will affect the filtration efficiency of the current DPF. Research showed that the PM discharged from the outlet of DPF in the active regeneration process increased by 2–3 orders of magnitude compared with that without regeneration [108]. The main reasons are as follows: Firstly, the deposited particles in DPF decrease with the oxidation and combustion of the deposited particles in DPF, resulting in low filtration efficiency and high particle penetration at the inlet; Secondly, the structure of the deposited soot layer changes, resulting in new or secondary particles escaping from DPF; and Thirdly, when the gaseous sulfuric acid leaves DPF system, the nucleating semi-volatile particles will be produced [51]. A series of research results showed that new or secondary particles were produced in the oxidation process of the soot layer, which was another reason for the increase in particles at the outlet of DPF, besides the leakage from the inlet flow [109]. Carlo et al. [110] conducted in-depth research on this phenomenon and found that a rapid temperature rise would aggravate the fragmentation of the sedimentary particle layer, while a stable temperature rise could make debris discharge more smoothly. PI et al. [10] modeled

the soot crushing phenomenon on the soot filtration model. A quasi two-dimensional extended DPF model including soot fragmentation was established. The phenomenon of dust fragmentation and its PN-FE filtration behavior are described. This section will introduce several common DPF active regeneration methods: Heating regeneration, Fuel combustion, Oxidative regeneration, and electrical devices (heaters or microwaves).

4.1.1. Heating Regeneration

When the exhaust temperature reaches 600 °C, 85% of the particle matters in the particulate filter are quickly oxidated to CO₂, and the other particles are oxidated to CO due to inadequate combustion caused by the lack of oxygen. In order to improve the exhaust temperature, the intake throttle can be used, the intake volume is reduced, and the exhaust flow is reduced, so as to meet the needs of regeneration. However, excessive intake throttling will greatly reduce oxygen concentration, increase PM, and reduce power and fuel economy performance. In addition, exhaust throttling, delaying injection time, and heating intake air can also be used to improve the exhaust temperature, but these methods will cause other new problems, such as excessive fuel consumption. Deng et al. [111] studied the distribution of DPF exhaust temperature based on the field synergy theory. It was concluded that when the exhaust flow of the DPF was 20–30 g/s and the soot load was less than 5 g/L, it was conducive to DPF regeneration. Deng et al. [112] put forward a new idea with the reciprocating flow on the reasonable temperature distribution in DPF regeneration: the ash could be blown away in the direction of the discharged pollutants and a small amount of additional heat energy could realize regeneration.

4.1.2. Fuel Combustion

The exhaust temperature of the diesel engine is very low at low speed and low load. The exhaust temperature is less than 150 °C at idle speed. At this time, the PM in the exhaust gas cannot reach the combustion temperature and it is impossible to burn and regenerate. In order to improve the exhaust temperature greatly, the fuel combustion regeneration method can be used. The working principle of this method is to set a burner at the entrance of the particle catcher, supply a small amount of fuel oil to the burner, use oxygen or other air supplied in the exhaust gas, and ignite the gas with a spark plug or glow plug, and then ignite the particles with high-temperature gas. Generally, the regeneration process can be completed after 1–2 min when the burner stops working. There were also studies supporting the use of post-injection technology to increase the amount of unburned fuel in exhaust gases. Excess fuel reacts in the diesel oxidation catalyst (DOC) to increase the temperature of the exhaust gas entering the DPF [113]. In this way, the exhaust gas temperature at the DOC outlet can reach above 600 °C, which meets the requirement of DPF active regeneration [114]. Pu has also proved that non-thermal plasma injection can be used to burn carbon deposits to complete regeneration during engine shutdown [115]. Dae combined hydrogen to propose a plasma burner, which could generate a stable flame through the continuous discharge and partial oxidation of fuel to realize regeneration. While removing PM, it also had a certain purification effect on CO, NO, and other emissions [116].

4.1.3. Electric Heating Regeneration

Electric heating regeneration is a relatively simple way to increase the temperature of exhaust gas and achieve regeneration and can be applied to most filter materials. After working for a period of time, electric heating regeneration uses an electric heating wire or other electric heating methods to periodically heat the particle filter to make the particles burn. The power of an electric heating regeneration system is generally between 3–6 kW, which is simple structure, convenient, safe, and reliable. Some studies have found that the use of 21 pairs of non-uniform dielectric barrier discharge (DBD) reactors can improve the energy efficiency of PM removal. When 90 W of energy is injected, 90% of PM can be

removed by plasma discharge [117]. The basic structure of an inhomogeneous DBD reactor is shown in Figure 9.

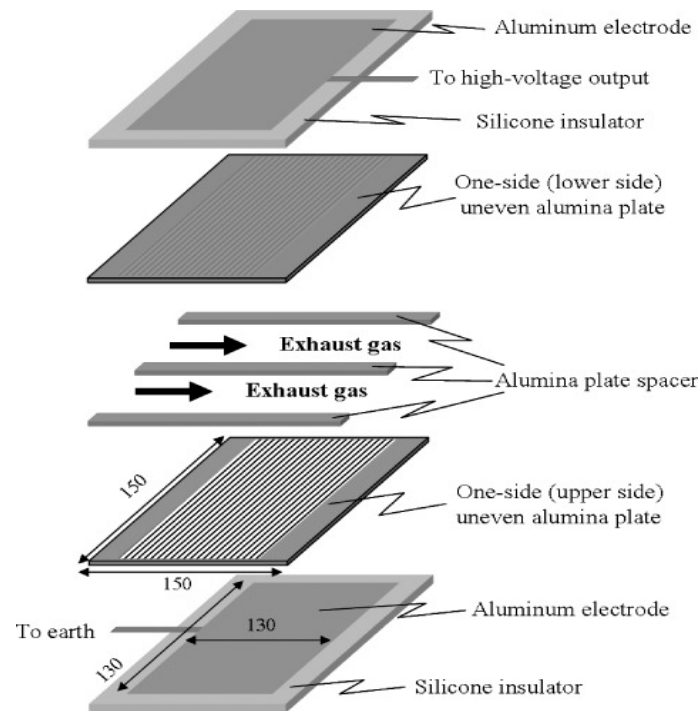


Figure 9. The basic structure of an inhomogeneous DBD reactor [117].

However, the heat utilization rate and regeneration rate are low, and the energy consumption is high. Therefore, electric heating is generally used together with a catalyst to solve the emission problem during the vehicle cold start process [118]. Gao studied different electric heating catalyst strategies and found that the electric heating method could reduce CO and HC emissions by 50% in the cold start process [119].

4.1.4. Microwave Regeneration

Microwave regeneration is the regeneration of particulates trapped by using the unique selective heating and volume heating characteristics of the microwave. Particles can absorb microwaves with a frequency of 2–10 GHz with an energy efficiency of 60%–70%. As the loss coefficient of ceramic is very low, the microwave does not heat the ceramic filter.

In the regeneration process, the temperature gradient inside the filter body is small, and the regeneration process is easy to control. Microwave regeneration has high efficiency and no secondary pollution. E et al. [120] modeled the microwave regeneration process of the microwave regeneration function DPF. It was found that the exhaust gas velocity had a significant effect on the regeneration performance, and the DPF structure was most conducive to microwave regeneration. At the same time, they also used the field synergy theory to optimize the parameters of the microwave-assisted regeneration system. It was concluded that when the inlet pressure was 0.08 MPa, it could have a good synergy with the maximum average temperature, which was conducive to the regeneration process [121]. Sameer et al. [122] studied the reliability of microwave active regeneration. Although there is no obvious physical damage to DPF after 150 filtration/regeneration cycles, the efficiency of active regeneration is not as high as that of passive regeneration. In Palma's experiment, the microwave absorption capacity increased with the increase in catalyst load. The experimental results are shown in Figure 10.

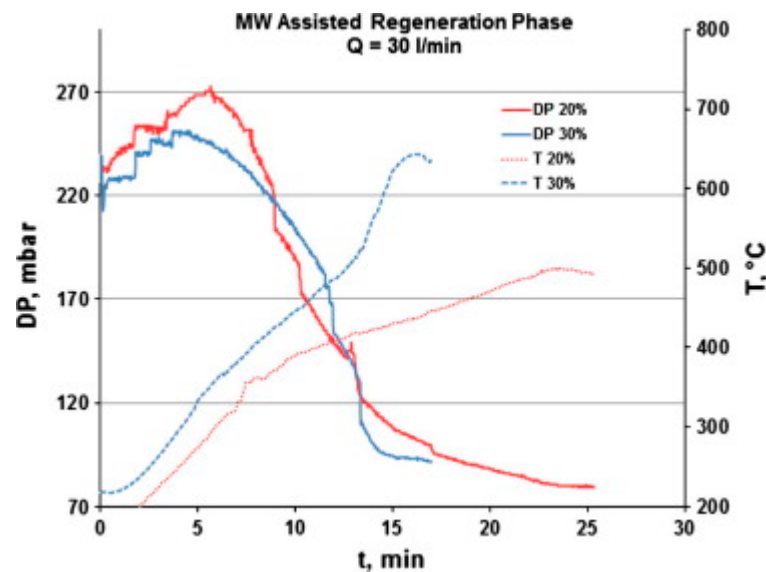


Figure 10. The behavior of the pressure drop through the filter (DP) and temperature profiles during the regeneration phase performed by the microwave generator set at 50% of nominal power and with an exhaust gas flow rate of $30 \text{ L}/\text{min}^{-1}$ [123].

4.2. Passive Regeneration

Passive regeneration is a process that uses the temperature of exhaust gas to make the PM in exhaust gas reach the ignition point and burn up themselves to generate harmless H_2O and CO_2 . In general, it is difficult for the exhaust gas to reach the combustion temperature of particles. Thus, a chemical catalyst is often used to reduce the chemical activity of particles to achieve regeneration [124].

Adding additives to fuel oil is a research hotspot of passive regeneration. Additives are generally soluble metals. The metal oxides generated after combustion with fuel will catalyze the particles, thus reducing the combustion temperature of the particles. In this way, even at a lower exhaust temperature, particles can spontaneously ignite without the aid of other external combustion equipment or energy [125].

However, some of the combustion products of the additive metal oxides will deposit like particles when they pass through the filter, blocking the gap of the filter body. Over time, this will affect the filter life, reduce the capture efficiency, and affect the power and economy of the diesel engine. At the same time, metal dust entering the atmosphere will cause secondary pollution to the environment which is also a problem to be considered in passive regeneration.

4.2.1. Oxidation Catalytic Regeneration

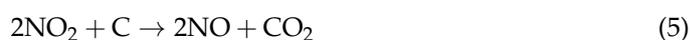
Oxidation catalytic regeneration uses catalysts to reduce the chemical activation energy of hydrocarbons, carbon monoxide, and SOF in diesel engine exhaust so that these substances can also react with O_2 to form CO_2 and H_2O at low exhaust temperatures.

Catalysts commonly used in diesel engines include perovskite-type oxides, crystalloid-type oxides, alkaline or heavy metal oxides, halide mixtures containing vanadate or molybdate, and precious metals [126]. In recent years, gold has been considered a better catalyst. It has better activation efficiency in the process of CO oxidation at low temperatures. However, the activation efficiency of gold depends to a great extent on its size. The smaller the size of gold particles, the better the activity. Caroca et al. [127] compared several DPFs and found that a nanostructured perovskite catalyst (LA—K—Cu—FeO) could complete the regeneration with lower energy consumption. Yi et al. [128] observed regeneration by attaching potassium titanate whiskers to cordierite and found that it successfully reduced the combustion activation energy of carbon particles.

However, the catalyst can play a better effect only when the diesel engine is fueled with low sulfur fuel. In general, its sulfur content should be less than 0.005%, even less than 0.001%. The sulfur in fuel oil will form sulfate after combustion. It will cover the inner surface of the oxidation catalyst and make the oxidation catalyst lose activity and reduce conversion efficiency.

4.2.2. Catalytic Regeneration

CDPFs have been proven as a more effective method than normal DPFs, coating catalysts on the surface of the filter body. The most commonly used commercial catalyst particles are Platinum, Palladium, and Rhodium (Pt, Pd, and Rh) which can attain lower soot oxidation temperatures [129,130]. When the exhaust temperature reaches about 400 °C, the particles will be oxidized. The reaction equations of the catalytic regeneration principle are as follows [131]:



The main disadvantages of catalytic regeneration are: (1) The contact reaction between solid particles and catalyst is so uneven that it is difficult to regenerate completely. (2) With the passage of time, the role of the catalyst will gradually weaken or even completely disappear, that is, catalyst poisoning will occur.

Kong et al. [132] simulated numerically the soot deposition and pressure in CDPF and DPF by a lattice Boltzmann method (LBM), and the following conclusions were reached: (1) There was more pressure at the area where the filter was catalyzed. (2) The in-wall CDPF had a larger pressure drop than that of the bare CDPF. (3) Compared to the in-wall CDPF, the on-wall CDPF had a larger soot deposition amount and showed a smaller pressure drop. The variation of soot content and pressure drop over time is shown in Figure 11. This means that more deposited soot can contact the catalyst layer in the on-wall CDPF and improve the efficiency of filter regeneration. There is also great interest in mixed catalysts. Some studies showed that a Pt/H-ZSM₅ mixture could improve the soot oxidation efficiency [133]. Duck et al. [134] found that the mixed catalysts of platinum, tungsten, and TiO₂ also had strong catalytic activity for NO.

4.3. Composite Regeneration

The third type of DPF regeneration system utilizes the combination of passive regeneration and active regeneration, that is to say, the catalyst is also equipped with an active regeneration system. According to the current experimental research, passive regeneration alone cannot deal with all working conditions flexibly. For example, in the process of highway driving, vehicles equipped with CDPF can regenerate passively. However, when they need to drive slowly in the city, they rely on active regeneration. In a word, the research and application of passive-active combinations regeneration are also very important.

E et al. [135] used a microwave heating composite regeneration system that includes a DPF and a microwave generator. In this test, microwave-assisted composite regeneration can save about 24% and 48% energy compared with microwave regeneration and fuel post-injection regeneration.

At present, many researchers are investigating the continuous regeneration technology [136–139] of DPFs. For example, Palma et al. [119] investigated the performance of a SiC foam filter during microwave regeneration with and without a catalyst coating.

Some researchers [140–144] have investigated other factors to reveal the thermodynamic and kinetic mechanisms of low-temperature combustion of the soot by NO₂. In conclusion, CR-DPF based on NO₂-assisted regeneration has become an advanced regeneration technology.

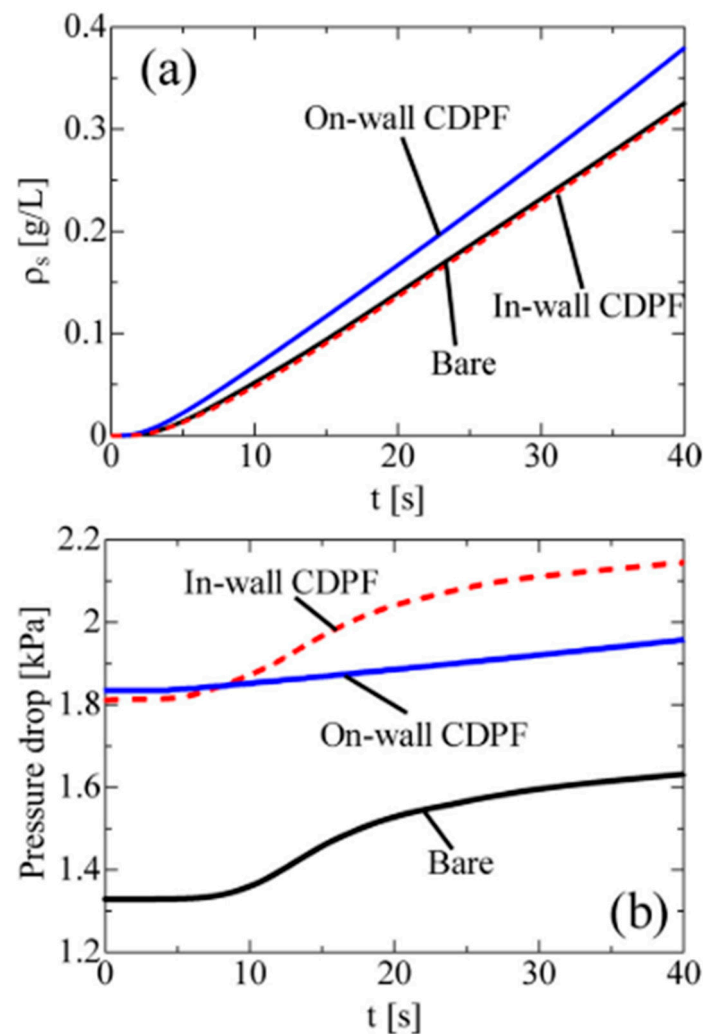


Figure 11. Time-variations of (a) soot amount and (b) pressure drop [132].

4.4. Pressure Drop

The engine back pressure produced by DPF installation is an important parameter of DPF, which directly affects the fuel economy of the engine. If the engine's back pressure is high, the engine must provide additional p-V work to overcome the increase in back pressure which will lead to poor combustion and higher fuel consumption by the engines [145]. Therefore, the different back pressure levels caused by the different DPFs can directly lead to different fuel consumption levels. The main task of optimization is to reduce the soot and pressure drop of the ash filter as much as possible without reducing the performance of a clean filter.

The design of the channel in DPF has always been the top priority in optimization. Studies showed that hexagonal channels had a lower pressure drop than commercially available square channels under controlled regeneration [125]. The hexagon channel also shows better thermal durability under uncontrolled regeneration [146]. At the same time, under the high-temperature condition of active regeneration, the pressure drop of asymmetric cell technology is lower than that of symmetric cell technology [147]. The optimization of design has an obvious improvement effect on the pressure drop of DPF. In recent years, the trend of a diesel mixture as an alternative energy to diesel is becoming more and more obvious. In addition to high environmental benefits, the mixture also has good performance in the regeneration process of DPFs. Some studies have shown that the regeneration pressure drop of a diesel/polyoxymethylene dimethyl ether mixture was significantly lower than that of pure diesel [125]. At the same time, the diesel additives

have also been proved to be effective in reducing pressure drop. When observing the regeneration process of diesel with Fuel Borne Catalyst (FBC), compared with the diesel without FBC, the pressure drop had an obvious downward trend [148]. The test results obtained by Xiao et al. [149] in Figure 12 show that the pressure drops decrease with the decrease in wall thickness, so it is an effective way to control the exhaust back pressure of the engine. In addition, E et al. [96] analyzed the pressure drop of the continuous regeneration-diesel particulate filter (CR-DPF) based on NO₂ assisted regeneration and found that the larger exhaust flow rate and high exhaust temperature can increase the initial pressure drop of the CR-DPF.

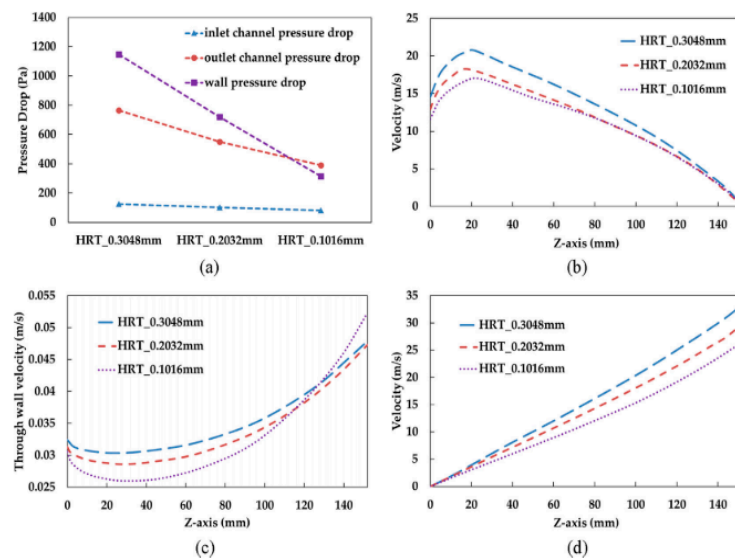


Figure 12. Flow and pressure drop characteristics of HRT with different wall thicknesses under a clean wall condition: (a) Pressure drop composition; (b) Inlet channel velocity; (c) Wall penetration velocity; and (d) Outlet channel velocity [149].

4.5. Soot Deposition

Take the most popular wall-flow DPF in the market as an example. The diameter of the PM is generally smaller than the filter aperture, so the soot deposition cannot be simplified to ordinary interception [150]. The soot deposition process on the DPF can be divided into four stages including the deep bed deposition stage, particle tree growth stage, particle tree connection stage, and soot cake layer stage [129]. Most of the non-uniform porous particle cake layers can be deposited from 130 μm to 500 μm [151].

In the past, the two main sedimentary stages (deep bed filtration and soot cake layer) were accurately modeled [47,152]. PM in the deep bed filtration stage is not affected by a single filtration mechanism, but by a mixture of multiple mechanisms [51]. The drag force, particle inertia, and Brownian motion are considered to be the main deposition mechanisms [153]. It is worth noting that ashes smaller than PM have been highlighted in recent studies. Ash first forms solid nanoparticles and then attaches to soot primary particles via agglomeration. Then, the aggregate is captured when it is transferred to the filter under the action of lift F_L , gravity G [154], resistance F_D , increasing mass force F_V , and adhesion force F_A (F_A includes van der Waals force [155], capillary force, chemical bonding force, and possible electrostatic force). The particle handling process is shown in Figure 13 [156]. Individually unabsorbed particles receive multiple forces in the pipe and eventually lead to the capture of most of the free ashes on the filter wall.

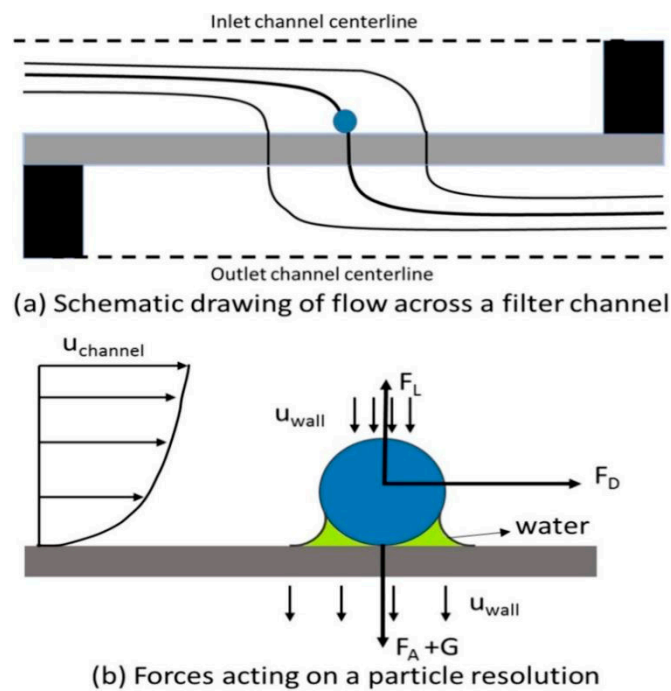


Figure 13. Force on particles [156].

After a few minutes of deep filtration, enough particulate matter accumulates in the channels to block the gaps and deposit an “impermeable” layer of soot on the filter wall. This stage is called the “cake filtration” stage. The pressure drop at this stage depends on its geometry, including soot bulk density, pipe thickness, and permeability [152]. Due to fuel economy issues, DPF needs to be regenerated periodically at this stage [10].

5. Gasoline Particulate Filter

5.1. Research Background of Gasoline Particulate Filter

Although the PM emission quality of gasoline engines is not as much as that of diesel engines, their emission quantity is roughly the same [157]. In addition, in terms of particle size, gasoline combustion produces smaller particles. These submicron particles with a diameter of less than 100 nm are more harmful to humans and animals [158]. Therefore, the particulate matter emission of gasoline vehicles has gradually attracted attention.

The mixture mode of the gasoline direct injection (GDI) engine is similar to that of the diesel engine. Unlike the traditional gasoline engine, it produces particles more easily. The number of particles emitted by GDI reaches 10^{13} #/km, which is higher than the Euro VI standard in 2014×10^{11} #/km [159]. In terms of emissions, China, Europe, and the United States all require a PM quality lower than 0.0045 g/km, which is a great challenge for GDI engines [160]. In addition to the unburned organic carbon particles, there may be volatile particles such as nitrate and sulfate in the steam or liquid phase in the exhaust gas of a GDI engine [161]. The main factors for the formation of soot particles are the mixture concentration and high temperature [162]. It is very difficult to form the same mixture with a homogeneous premixed gasoline engine in the way of direct injection in the cylinder, and the fuel adhesion in the cylinder will also create the partially rich mixture. For the GDI engine, PM emission is a problem that must be solved.

In order to meet stringent regulations, the technology of PM emission control of gasoline engines is constantly improving. The common technologies are fuel mixture and alternative fuel [159,163], exhaust gas after-treatment [164], and fuel injection strategy [165]. GPF is one of the most significant, which can help gasoline engine emissions meet Euro VI standards [166].

5.2. Causes of Particles in Gasoline Engine

The main fuel injection is completed in the intake and compression stroke before ignition [167]. Compared with the air inlet injection, the evaporation and atomization time of fuel are reduced. The fuel may still exist in the form of droplets during the ignition and combustion processes. Compared with gaseous fuel, liquid fuel produces more particles. Secondly, when the fuel is injected into the cylinder, it is possible that the fuel may be injected into the cylinder wall or on top of the piston. Because the temperatures of the cylinder wall and piston top are lower than that of the combustion chamber, the fuel-injected into these positions does not easily to burn completely, thus producing particles. In order to make the atomization effect of injected fuel better, the fuel injection pressure reaches 200 atmospheres. However, the generation of particles cannot be completely avoided [168]. The particulate matter emission of the gasoline engine is very low compared with diesel engine, but the national limit of particulate matter emission of the gasoline engine is also very low, only 4.5 mg/km. For the traditional direct injection gasoline engine, the gasoline particulate filter (GPF) is an essential after-treatment device [7]. Vehicles with GPF can reduce particulate matter emissions by about 90% in one test cycle compared with vehicles without GPF [169].

With the increasing awareness of environmental protection, more and more strict regulations on vehicle emission limits were proposed by national organizations. For environmental safety, it is an inevitable trend for the new cars produced by major car factories to use GPF. This paper mainly introduces the scheme of “after treatment”, that is, the particle catcher of the gasoline engine called GPF. The GPF collects the particles emitted by the engine and prevents them from entering the atmosphere.

5.3. Gasoline Particulate Filter Structure

The shape of GPF is a cylinder, which is no different from our traditional DOC shape. Therefore, there are no new requirements for the vehicle chassis. Moreover, the internal filter channel is also similar to the honeycomb structure of DPF [170].

5.4. Gasoline Particulate Filter Working and Regeneration Principle

5.4.1. Working Principle of Gasoline Particulate Filter

At present, most GPFs adopt a wall-flow structure, and its working principle is shown in Figure 14a,b [171]. The thermal shock resistance of cordierite is very important for the particulate filter of a gasoline engine. Cordierite has better thermal shock resistance and a smaller coefficient of thermal expansion. Thus, the cordierite is very suitable as a material for the particle catcher of gasoline engines [172]. In addition, some studies reported that Silicon carbon (SiC) [173] and foam metals were also well qualified for GPF. However, the cordierite is still used in most of the existing GPFs. There are several parallel channels in cordierite carriers [174]. The exhaust gas of the engine flows in through the inlet channel and out of the adjacent channel. The soot particles inside the exhaust gas form a trap on the wall. When the amount of carbon smoke accumulates to a certain extent, a control strategy needs to be designed for oxidation regeneration.

5.4.2. Regeneration Principle of the Gasoline Particulate Filter

Particles will be trapped and collected when passing through the side wall, which is equivalent to filtration. In general, the GPF can capture 99% of particles. At the same time, regeneration occurs in the GPF. Particles trapped in the GPF will remain in it, which is equivalent to blocking the exhaust channel of the GPF. If too many particles are trapped, the exhaust resistance will increase and then the fuel consumption will increase, which is unfavorable [175].

When the vehicle runs at high speed, due to the high exhaust temperature, the particles will burn with the oxygen in the exhaust, which is the regeneration of GPF. GPF regeneration can be divided into two categories: active regeneration and passive regeneration. Active

regeneration needs to increase external conditions to promote regeneration and passive regeneration is the natural regeneration of the engine under normal conditions [176].

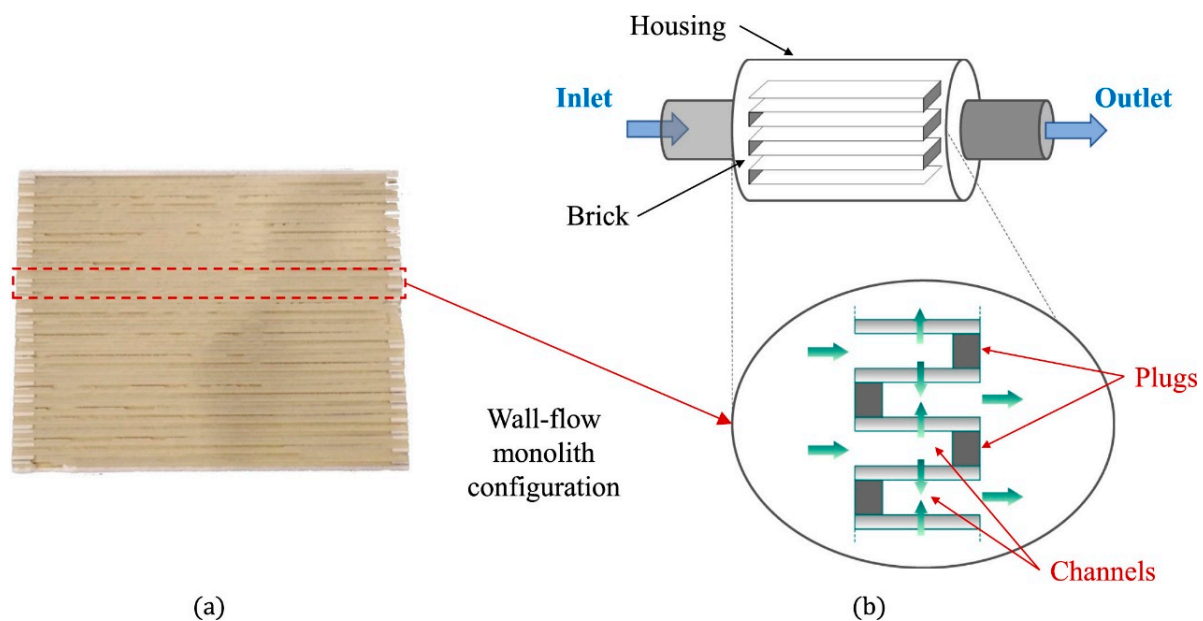


Figure 14. Working principle of GPF: (a) Wall-flow monolith structure; (b) Channel structure [171].

Active regeneration can be divided into enrichment oil cut-off regeneration, electric heating regeneration, microwave regeneration, infrared regeneration, blowback regeneration, and vibration regeneration. Passive regeneration is divided into adding catalyst into the fuel oil [177] and coating catalyst on the support [171,178].

6. Conclusions

With the continuous deterioration of energy crisis [179–185] and environmental problems [186–190], how to effectively reduce engine emissions is the main area of interest for researchers today. DPFs are considered to be one of the most effective means to solve the high PM emission of diesel engines. However, today's DPF development has not reached the desired level. For example, ashes from fuel, engine wear, and lubricants cannot be removed by ordinary regeneration, which will “permanently” block the filter channels. Although it can be eliminated by uncontrolled regeneration, such a cost will irreversibly damage the DPF substrate and reduce its lifetime [29]. In addition, the high pressure drop during operation has an impact on fuel economy and driving safety. These problems are being overcome by filter structure, catalyst, and more perfect regeneration control. The optimization of the DPF has a very positive impact on the number of discharged particles, particle size, exhaust pressure drops, energy consumption, and filtration/regeneration efficiency.

At present, the difficulty of DPFs is mainly to infer a DPF operation and regeneration strategy according to the DPF soot load. Considering active regeneration, how to balance the optimal efficiency of regeneration and soot deposition will become the key problem to be solved. The introduction of GPFs may be the best way to solve the problem. Although the current performance of GPFs can meet regulation requirements, in the long run, how to further reduce the pressure drop and improve the filtration efficiency is the primary task of optimizing GPFs. These results will directly affect the market share of vehicles equipped with GDI engines.

The above research shows a good foundation for the study of DPF regeneration, however, there are still some problems that remain unclear:

- (1) The formation mechanism of new or secondary particles in soot oxidation is not clear.

- (2) The interaction of the mechanism of soot oxidation is not clear concerning the emission characteristics of PM and between particulate sources.
- (3) The factors influencing the emission characteristics of PM need to be further explored.

Future studies must research the mechanism of soot layer thickness changing during the regeneration process, the specific thickness of irregular soot layer scallops in the middle of the II-regeneration stage, and the thin soot layer at the III-regeneration stage. The effects of oxygen concentration and additional NO₂ on the soot layer substrate structure should be investigated by measuring its downstream concentrations when the soot layer begins to oxidize [44].

Author Contributions: Conceptualization, Z.Z.; methodology, R.D., Z.Z. and Y.Y.; software, R.D.; validation, Z.Z. and Y.Y.; formal analysis, R.D., Z.Z., Y.Y., H.H. and C.C.; investigation, H.H. and C.C.; resources, Z.Z.; data curation, R.D., Z.Z., and C.C.; writing—original draft preparation, R.D., Z.Z. and Y.Y.; writing—review and editing, Z.Z., Y.Y., H.H. and C.C.; visualization, R.D. and Z.Z.; supervision, Z.Z.; project administration, Z.Z.; funding acquisition, Z.Z. and Y.Y. All authors have read and agreed to the published version of the manuscript.

Funding: This research is supported by Guangxi Science and Technology Program Project (AB19110051), the Liuzhou Science and Technology Program(2019BA10601), the Innovation Project of Guangxi University of Science and Technology Graduate education under the research grants of GKYC202208.

Data Availability Statement: All data used to support the findings of this study are included within the article.

Acknowledgments: This research is supported by Guangxi Science and Technology Program Project (AB19110051), the Liuzhou Science and Technology Program(2019BA10601), the Innovation Project of Guangxi University of Science and Technology Graduate education under the research grants of GKYC202208. We also would like to thank all the reviewers for providing valuable comments.

Conflicts of Interest: The authors declare that there is no conflict of interest regarding the publication of this paper.

References

1. Zhao, D.; Li, L. Effect of choked outlet on transient energy growth analysis of a thermoacoustic system. *Appl. Energy* **2015**, *160*, 502–510. [[CrossRef](#)]
2. Chen, P.; Ibrahim, U.; Wang, J. Experimental investigation of diesel and biodiesel post injections during active diesel particulate filter regenerations. *Fuel* **2014**, *130*, 286–295. [[CrossRef](#)]
3. Cai, T.; Zhao, D.; Sun, Y.; Ni, S.; Li, W.; Guan, D.; Wang, B. Evaluation of NO_x emissions characteristics in a CO₂-Free micro-power system by implementing a perforated plate. *Renew. Sustain. Energy Rev.* **2021**, *145*, 111150. [[CrossRef](#)]
4. Zhang, Z.; Tian, J.; Li, J.; Lv, J.; Wang, S.; Zhong, Y.; Dong, R.; Gao, S.; Cao, C.; Tan, D. Investigation on combustion, performance and emission characteristics of a diesel engine fueled with diesel/alcohol/n-butanol blended fuels. *Fuel* **2022**, *320*, 123975. [[CrossRef](#)]
5. Xie, B.; Peng, Q.; Yang, W.; Li, S.; E, J.; Li, Z.; Tao, M.; Zhang, A. Effect of pins and exit-step on thermal performance and energy efficiency of hydrogen-fueled combustion for micro-thermophotovoltaic. *Energy* **2022**, *239*, 122341. [[CrossRef](#)]
6. Wang, B.; Mosbach, S.; Schmutzhard, S.; Shuai, S.; Huang, Y.; Kraft, M. Modelling soot formation from wall films in a gasoline direct injection engine using a detailed population balance model. *Appl. Energy* **2016**, *163*, 154–166. [[CrossRef](#)]
7. Fan, L.; Cheng, F.; Zhang, T.; Liu, G.; Yuan, J.; Mao, P. Visible-light photoredox-promoted desilylative allylation of α -silylamines: An efficient route to synthesis of homoallylic amines. *Tetrahedron Lett.* **2021**, *81*, 153357. [[CrossRef](#)]
8. Zhang, Z.; E, J.; Deng, Y.; Pham, M.; Zuo, W.; Peng, Q.; Yin, Z. Effects of fatty acid methyl esters proportion on combustion and emission characteristics of a biodiesel fueled marine diesel engine. *Energy Convers. Manag.* **2018**, *159*, 244–253. [[CrossRef](#)]
9. Cai, T.; Becker, S.M.; Cao, F.; Wang, B.; Tang, A.; Fu, J.; Han, L.; Sun, Y.; Zhao, D. NO_x emission performance assessment on a perforated plate-implemented premixed ammonia-oxygen micro-combustion system. *Chem. Eng. J.* **2021**, *417*, 128033. [[CrossRef](#)]
10. Giechaskiel, B.; Melas, A.; Lähde, T. Detailed Characterization of Solid and Volatile Particle Emissions of Two Euro 6 Diesel Vehicles. *Appl. Sci.* **2022**, *12*, 3321. [[CrossRef](#)]
11. Zhang, Z.; Li, J.; Tian, J.; Dong, R.; Zou, Z.; Gao, S.; Tan, D. Performance, combustion and emission characteristics investigations on a diesel engine fueled with diesel/ethanol/n-butanol blends. *Energy* **2022**, *249*, 123733. [[CrossRef](#)]
12. E, J.; Zhang, Z.; Chen, J.; Pham, M.; Zhao, X.; Peng, Q.; Zhang, B.; Yin, Z. Performance and emission evaluation of a marine diesel engine fueled by water biodiesel-diesel emulsion blends with a fuel additive of a cerium oxide nanoparticle. *Energy Convers. Manag.* **2018**, *169*, 194–205. [[CrossRef](#)]

13. Zhang, Z.; Tian, J.; Xie, G.; Li, J.; Xu, W.; Jiang, F.; Huang, Y.; Tan, D. Investigation on the combustion and emission characteristics of diesel engine fueled with diesel/methanol/n-butanol blends. *Fuel* **2022**, *314*, 123088. [[CrossRef](#)]
14. Hu, Y.; Sun, Y.; He, J.; Fang, D.; Zhu, J.; Meng, X. Effect of friction stir processing parameters on the microstructure and properties of ZK60 magnesium alloy. *Mater. Res. Express* **2022**, *8*, 016508. [[CrossRef](#)]
15. Peng, Q.; Xie, B.; Yang, W.; Tang, S.; Li, Z.; Zhou, P.; Luo, N. Effects of porosity and multilayers of porous medium on the hydrogen-fueled combustion and micro-thermophotovoltaic. *Renew. Energy* **2021**, *174*, 391–402. [[CrossRef](#)]
16. Tan, D.; Chen, Z.; Li, J.; Luo, J.; Yang, D.; Cui, S.; Zhang, Z. Effects of Swirl and Boiling Heat Transfer on the Performance Enhancement and Emission Reduction for a Medium Diesel Engine Fueled with Biodiesel. *Processes* **2021**, *9*, 568. [[CrossRef](#)]
17. Yan, Z.; Gainey, B.; Lawler, B. A parametric modeling study of thermal barrier coatings in low-temperature combustion engines. *Appl. Therm. Eng.* **2022**, *200*, 117687. [[CrossRef](#)]
18. Shi, Y.; Cai, Y.; Li, X.; Pu, X.; Zhao, N.; Wang, W. Effect of the amount of trapped particulate matter on diesel particulate filter regeneration performance using non-thermal plasma assisted by exhaust waste heat. *Plasma Sci. Technol.* **2020**, *22*, 15504. [[CrossRef](#)]
19. Zhou, L.; Hallquist, Å.M.; Hallquist, M.; Salvador, C.M.; Gaita, S.M.; Sjödin, Å.; Jerksjö, M.; Salberg, H.; Wängberg, I.; Mellqvist, J.; et al. A transition of atmospheric emissions of particles and gases from on-road heavy-duty trucks. *Atmos. Chem. Phys.* **2020**, *20*, 1701–1722. [[CrossRef](#)]
20. Cai, T.; Zhao, D. Temperature Dependence of Laminar Burning Velocity in Ammonia/Dimethyl Ether-air Premixed Flames. *J. Therm. Sci.* **2022**, *31*, 189–197. [[CrossRef](#)]
21. Gainey, B.; Yan, Z.; Lawler, B. Autoignition characterization of methanol, ethanol, propanol, and butanol over a wide range of operating conditions in LTC/HCCI. *Fuel* **2021**, *287*, 119495. [[CrossRef](#)]
22. Zheng, X.; Wu, Y.; Zhang, S.; Baldauf, R.W.; Zhang, K.M.; Hu, J.; Li, Z.; Fu, L.; Hao, J. Joint measurements of black carbon and particle mass for heavy-duty diesel vehicles using a portable emission measurement system. *Atmos. Environ.* **2016**, *141*, 435–442. [[CrossRef](#)]
23. E, J.; Xie, L.; Zuo, Q.; Zhang, G. Effect analysis on regeneration speed of continuous regeneration-diesel particulate filter based on NO₂-assisted regeneration. *Atmos. Pollut. Res.* **2016**, *7*, 9–17. [[CrossRef](#)]
24. Liu, H.; Xie, M.; Wu, D. Thermodynamic analysis of the heat regenerative cycle in porous medium engine. *Energy Convers. Manag.* **2009**, *50*, 297–303. [[CrossRef](#)]
25. You, H.; Gao, R.; Hu, P.; Liang, K.; Zhou, X.; Huang, X.; Pan, M. Sensitivity analysis of diesel particulate filters to geometric parameters during soot loading and its multi-objective optimization. *Process Saf. Environ. Prot.* **2022**, *159*, 251–265. [[CrossRef](#)]
26. Jung, D.; Bang, J.; Choi, S.; Choi, H.; Min, K. Optimization algorithm for diesel engine operating parameters based on a vehicle driving test cycle. *J. Mech. Sci. Technol.* **2013**, *27*, 2171–2179. [[CrossRef](#)]
27. Gainey, B.; O'Donnell, P.; Yan, Z.; Moser, S.; Lawler, B. LTC performance of C1–C4 water-alcohol blends with the same cooling potential. *Fuel* **2021**, *293*, 120480. [[CrossRef](#)]
28. Ge, J.C.; Kim, H.Y.; Yoon, S.K.; Choi, N.J. Reducing volatile organic compound emissions from diesel engines using canola oil biodiesel fuel and blends. *Fuel* **2018**, *218*, 266–274. [[CrossRef](#)]
29. Guan, B.; Zhan, R.; Lin, H.; Huang, Z. Review of the state-of-the-art of exhaust particulate filter technology in internal combustion engines. *J. Environ. Manag.* **2015**, *154*, 225–258. [[CrossRef](#)]
30. Meng, Z.; Chen, C.; Li, J.; Fang, J.; Tan, J.; Qin, Y.; Jiang, Y.; Qin, Z.; Bai, W.; Liang, K. Particle emission characteristics of DPF regeneration from DPF regeneration bench and diesel engine bench measurements. *Fuel* **2020**, *262*, 116589. [[CrossRef](#)]
31. Wei, Y.; Wang, K.; Wang, W.; Liu, S.; Chen, X.; Yang, Y.; Bai, S. Comparison study on the emission characteristics of diesel-and dimethyl ether-originated particulate matters. *Appl. Energy* **2014**, *130*, 357–369. [[CrossRef](#)]
32. Millo, F.; Vlachos, T.; Piano, A. Physicochemical and mutagenic analysis of particulate matter emissions from an automotive diesel engine fuelled with fossil and biofuel blends. *Fuel* **2021**, *285*, 119092. [[CrossRef](#)]
33. Mohankumar, S.; Senthilkumar, P. Particulate matter formation and its control methodologies for diesel engine: A comprehensive review. *Renew. Sustain. Energy Rev.* **2017**, *80*, 1227–1238. [[CrossRef](#)]
34. Caroca, J.C.; Millo, F.; Vezza, D.; Vlachos, T.; De Filippo, A.; Bensaid, S.; Russo, N.; Fino, D. Detailed Investigation on Soot Particle Size Distribution during DPF Regeneration, using Standard and Bio-Diesel Fuels. *Ind. Eng. Chem. Res.* **2010**, *50*, 2650–2658. [[CrossRef](#)]
35. Cai, T.; Zhao, D. Enhancing and assessing ammonia-air combustion performance by blending with dimethyl ether. *Renew. Sustain. Energy Rev.* **2022**, *156*, 112003. [[CrossRef](#)]
36. Ge, J.C.; Kim, H.Y.; Yoon, S.K.; Choi, N.J. Optimization of palm oil biodiesel blends and engine operating parameters to improve performance and PM morphology in a common rail direct injection diesel engine. *Fuel* **2020**, *260*, 116326. [[CrossRef](#)]
37. Fische, J.; Zheng, Y.; Lyu, T.; Bian, J.; Hu, H. Environmental effects on acute exacerbations of respiratory diseases: A real-world big data study. *Sci. Total Environ.* **2022**, *806*, 150352. [[CrossRef](#)]
38. Pu, X.; Wang, L.; Chen, L.; Pan, J.; Tang, L.; Wen, J.; Qiu, H. Differential effects of size-specific particulate matter on lower respiratory infections in children: A multi-city time-series analysis in Sichuan, China. *Environ. Res.* **2021**, *193*, 110581. [[CrossRef](#)]
39. Wang, Y.; Xiong, L.; Huang, X.; Ma, Y.; Zou, L.; Liang, Y.; Xie, W.; Wu, Y.; Chang, X.; Wang, Z.; et al. Intermittent exposure to airborne particulate matter induces subcellular dysfunction and aortic cell damage in BALB/c mice through multi-endpoint assessment at environmentally relevant concentrations. *J. Hazard. Mater.* **2022**, *424*, 127169. [[CrossRef](#)]

40. Miller, M.R. The cardiovascular effects of air pollution: Prevention and reversal by pharmacological agents. *Pharm. Ther.* **2022**, *232*, 107996. [[CrossRef](#)]
41. Zhou, S.; Zhu, Q.; Liu, H.; Jiang, S.; Zhang, X.; Peng, C.; Yang, G.; Li, J.; Cheng, L.; Zhong, R.; et al. Associations of polycyclic aromatic hydrocarbons exposure and its interaction with XRCC1 genetic polymorphism with lung cancer: A case-control study. *Environ. Pollut.* **2021**, *290*, 118077. [[CrossRef](#)] [[PubMed](#)]
42. Liu, H.; Liao, J.; Jiang, Y.; Zhang, B.; Yu, H.; Kang, J.; Hu, C.; Li, Y.; Xu, S. Maternal exposure to fine particulate matter and the risk of fetal distress. *Ecotoxicol. Environ. Saf.* **2019**, *170*, 253–258. [[CrossRef](#)] [[PubMed](#)]
43. Wei, J.; Li, Z.; Lyapustin, A.; Sun, L.; Peng, Y.; Xue, W.; Su, T.; Cribb, M. Reconstructing 1-km-resolution high-quality PM_{2.5} data records from 2000 to 2018 in China: Spatiotemporal variations and policy implications. *Remote Sens. Environ.* **2021**, *252*, 112136. [[CrossRef](#)]
44. Wu, Y.; Wang, P.; Farhan, S.M.; Yi, J.; Lei, L. Effect of post-injection on combustion and exhaust emissions in DI diesel engine. *Fuel* **2019**, *258*, 116131. [[CrossRef](#)]
45. Feng, S.; Hong, W.; Yao, Y.; You, T. Research of Post Injection Strategy of an EGR Diesel Engine to Improve Combustion and Particulate Emissions Performance: Application on the Transient Operation. *Symmetry* **2020**, *12*, 3390. [[CrossRef](#)]
46. Kontses, A.; Dimaratos, A.; Keramidis, C.; Williams, R.; Hamje, H.; Ntziachristos, L.; Samaras, Z. Effects of fuel properties on particulate emissions of diesel cars equipped with diesel particulate filters. *Fuel* **2019**, *255*, 115879. [[CrossRef](#)]
47. Guo, Y.; Stevanovic, S.; Verma, P.; Jafari, M.; Jabbour, N.; Brown, R.; Cravigan, L.; Alroe, J.; Osuagwu, C.G.; Brown, R.; et al. An experimental study of the role of biodiesel on the performance of diesel particulate filters. *Fuel* **2019**, *247*, 67–76. [[CrossRef](#)]
48. Liu, J.; Ulishney, C.J.; Dumitrescu, C.E. Experimental investigation of a heavy-duty natural gas engine performance operated at stoichiometric and lean operations. *Energy Convers. Manag.* **2021**, *14*, 335–344. [[CrossRef](#)]
49. Kim, K.H.; Choi, B.; Park, S.; Kim, E.; Chiaramonti, D. Emission characteristics of compression ignition (CI) engine using diesel blended with hydrated butanol. *Fuel* **2019**, *257*, 116037. [[CrossRef](#)]
50. Ge, J.C.; Wu, G.; Choi, N.J. Comparative study of pilot–main injection timings and diesel/ethanol binary blends on combustion, emission and microstructure of particles emitted from diesel engines. *Fuel* **2022**, *313*, 122658. [[CrossRef](#)]
51. Lao, C.T.; Akroyd, J.; Eaves, N.; Smith, A.; Morgan, N.; Bhave, A.; Kraft, M. Modelling particle mass and particle number emissions during the active regeneration of diesel particulate filters. *Proc. Combust. Inst.* **2019**, *37*, 4831–4838. [[CrossRef](#)]
52. Choi, S.; Oh, K.-C.; Lee, C.-B. The effects of filter porosity and flow conditions on soot deposition/oxidation and pressure drop in particulate filters. *Energy* **2014**, *77*, 327–337. [[CrossRef](#)]
53. Fang, J.; Meng, Z.; Li, J.; Pu, Y.; Du, Y.; Li, J.; Jin, Z.; Chen, C.; Chase, G.G. The influence of ash on soot deposition and regeneration processes in diesel particulate filter. *Appl. Therm. Eng.* **2017**, *124*, 633–640. [[CrossRef](#)]
54. Park, J.K.; Nguyen, T.H.; Kim, C.N.; Lee, S.Y. Simulation of flow in diesel particulate filter system using metal fiber filter media. *Int. J. Automot. Technol.* **2014**, *15*, 361–367. [[CrossRef](#)]
55. Li, Z.; Yan, F.; Kong, X.; Shen, B.; Li, Z.; Wang, Y. Simulation of soot particle deposition inside porous walls based on lattice Boltzmann method for diesel particulate filter. *J. Environ. Chem. Eng.* **2021**, *9*, 105396. [[CrossRef](#)]
56. Wang, D.-Y.; Tan, P.-Q.; Zhu, L.; Wang, Y.-H.; Hu, Z.-Y.; Lou, D.-M. Novel soot loading prediction model of diesel particulate filter based on collection mechanism and equivalent permeability. *Fuel* **2021**, *286*, 119409. [[CrossRef](#)]
57. Lao, C.T.; Akroyd, J.; Eaves, N.; Smith, A.; Morgan, N.; Nurkowski, D.; Bhave, A.; Kraft, M. Investigation of the impact of the configuration of exhaust after-treatment system for diesel engines. *Appl. Energy* **2020**, *267*, 114844. [[CrossRef](#)]
58. Liu, B.; Sun, P.; Aggarwal, S.K.; Zhao, S.; Huang, B. An experimental-computational study of DPF soot capture and heat regeneration. *Int. J. Green Energy* **2020**, *17*, 301–308. [[CrossRef](#)]
59. Yang, K.; Fox, J.T.; Hunsicker, R. Interaction of Na, K, and Fe with porous cordierite at elevated temperatures. *J. Mater. Sci.* **2016**, *52*, 4025–4041. [[CrossRef](#)]
60. Zhang, Z.; Wang, F.; Yu, X.; Wang, Y.; Yan, Y.; Li, K.; Luan, Z. Porous Silicon Carbide Ceramics Produced by a Carbon Foam Derived from Mixtures of Mesophase Pitch and Si Particles. *J. Am. Ceram. Soc.* **2009**, *92*, 260–263. [[CrossRef](#)]
61. Brodnik, N.R.; Faber, K.T. Out-of-plane mechanical characterization of acicular mullite and aluminum titanate diesel particulate filters. *Int. J. Appl. Ceram. Technol.* **2018**, *16*, 1173–1183. [[CrossRef](#)]
62. Wang, X.; Liu, C.; Li, J.; Qiao, L.; Bai, Y. Porous aluminum titanate–strontium feldspar–mullite fiber composite ceramics with enhanced pore structures and mechanical properties. *Ceram. Int.* **2018**, *44*, 22686–22691. [[CrossRef](#)]
63. Burteau, A.; N’Guyen, F.; Bartout, J.D.; Forest, S.; Bienvenu, Y.; Saberi, S.; Naumann, D. Impact of material processing and deformation on cell morphology and mechanical behavior of polyurethane and nickel foams. *Int. J. Solids Struct.* **2012**, *49*, 2714–2732. [[CrossRef](#)]
64. Adler, J. Ceramic Diesel Particulate Filters. *Int. J. Appl. Ceram. Technol.* **2005**, *2*, 429–439. [[CrossRef](#)]
65. Oh, Y.-J.; Oh, T.-S.; Jung, H.-J. Microstructure and mechanical properties of cordierite ceramics toughened by monoclinic ZrO₂. *J. Mater. Sci.* **1991**, *26*, 6491–6495. [[CrossRef](#)]
66. Han, W.; Yi, H.; Tang, X.; Zhao, S.; Gao, F.; Zhang, X.; Ma, C.; Song, L. Mn-Fe-Ce Coating onto Cordierite Monoliths as Structured Catalysts for NO Catalytic Oxidation. *ChemistrySelect* **2019**, *4*, 4664–4671. [[CrossRef](#)]
67. Yu, F.; Nie, W.; Zhou, W.; Yuan, M.; Yan, J.; Hua, Y.; Bao, Q.; Niu, W. Performance evaluation of Mn-Ce/cordierite catalyst modified by green surfactant to remove NO_x in underground mines at low temperatures. *J. Environ. Chem. Eng.* **2021**, *9*, 106499. [[CrossRef](#)]

68. Yildiz, I.; Caliskan, H.; Mori, K. Effects of cordierite particulate filters on diesel engine exhaust emissions in terms of pollution prevention approaches for better environmental management. *J. Environ. Manag.* **2021**, *293*, 112873. [[CrossRef](#)]
69. Chae, K.-W.; Son, M.-A.; Park, S.-J.; Kim, J.S.; Kim, S.-H. Effect of sintering atmosphere on the crystallizations, porosity, and thermal expansion coefficient of cordierite honeycomb ceramics. *Ceram. Int.* **2021**, *47*, 19526–19537. [[CrossRef](#)]
70. Ricca, A.; Palma, V.; Martino, M.; Meloni, E. Innovative catalyst design for methane steam reforming intensification. *Fuel* **2017**, *198*, 175–182. [[CrossRef](#)]
71. Benaqqa, C.; Gomina, M.; Beurotte, A.; Boussuge, M.; Delattre, B.; Pajot, K.; Pawlak, E.; Rodrigues, F. Morphology, physical, thermal and mechanical properties of the constitutive materials of diesel particulate filters. *Appl. Therm. Eng.* **2014**, *62*, 599–606. [[CrossRef](#)]
72. Yildiz, I.; Caliskan, H.; Mori, K. Energy, exergy and environmental assessments of biodiesel and diesel fuels for an internal combustion engine using silicon carbide particulate filter. *J. Therm. Anal. Calorim.* **2020**, *145*, 739–750. [[CrossRef](#)]
73. Zhang, B.; E, J.; Gong, J.; Yuan, W.; Zhao, X.; Hu, W. Influence of structural and operating factors on performance degradation of the diesel particulate filter based on composite regeneration. *Appl. Therm. Eng.* **2017**, *121*, 838–852. [[CrossRef](#)]
74. Fang, J.; Meng, Z.; Li, J.; Du, Y.; Qin, Y.; Jiang, Y.; Bai, W.; Chase, G.G. The effect of operating parameters on regeneration characteristics and particulate emission characteristics of diesel particulate filters. *Appl. Therm. Eng.* **2019**, *148*, 860–867. [[CrossRef](#)]
75. Ayodhya, A.S.; Narayanappa, K.G. An overview of after-treatment systems for diesel engines. *Environ. Sci. Pollut. Res. Int.* **2018**, *25*, 35034–35047. [[CrossRef](#)] [[PubMed](#)]
76. Tuler, F.E.; Portela, R.; Ávila, P.; Bortolozzi, J.P.; Miró, E.E.; Milt, V.G. Development of sepiolite/SiC porous catalytic filters for diesel soot abatement. *Microporous Mesoporous Mater.* **2016**, *230*, 11–19. [[CrossRef](#)]
77. Chiavola, O.; Chiatti, G.; Sirhan, N. Impact of Particulate Size during Deep Loading on DPF Management. *Appl. Sci.* **2019**, *9*, 3075. [[CrossRef](#)]
78. Zhao, X.; E, J.; Liao, G.; Zhang, F.; Chen, J.; Deng, Y. Numerical simulation study on soot continuous regeneration combustion model of diesel particulate filter under exhaust gas heavy load. *Fuel* **2021**, *290*, 119795. [[CrossRef](#)]
79. Zhang, Z.; Li, J.; Tian, J.; Zhong, Y.; Zou, Z.; Dong, R.; Gao, S.; Xu, W.; Tan, D. The effects of Mn-based catalysts on the selective catalytic reduction of NO_x with NH₃ at low temperature: A review. *Fuel Process. Technol.* **2022**, *230*, 107213. [[CrossRef](#)]
80. Zhang, Z.; Ye, J.; Tan, D.; Feng, Z.; Luo, J.; Tan, Y.; Huang, Y. The effects of Fe₂O₃ based DOC and SCR catalyst on the combustion and emission characteristics of a diesel engine fueled with biodiesel. *Fuel* **2021**, *290*, 120039. [[CrossRef](#)]
81. Lupše, J.; Campolo, M.; Soldati, A. Modelling soot deposition and monolith regeneration for optimal design of automotive DPFs. *Chem. Eng. Sci.* **2016**, *151*, 36–50. [[CrossRef](#)]
82. Tan, P.-Q.; Wang, D.-Y.; Yao, C.-J.; Zhu, L.; Wang, Y.-H.; Wang, M.-H.; Hu, Z.-Y.; Lou, D.-M. Extended filtration model for diesel particulate filter based on diesel particulate matter morphology characteristics. *Fuel* **2020**, *277*, 118150. [[CrossRef](#)]
83. Apicella, B.; Mancaruso, E.; Russo, C.; Tregrossi, A.; Oliano, M.M.; Ciajolo, A.; Vaglieco, B.M. Effect of after-treatment systems on particulate matter emissions in diesel engine exhaust. *Exp. Therm. Fluid Sci.* **2020**, *116*, 110107. [[CrossRef](#)]
84. Shi, Y.; Cai, Y.; Fan, R.; Cui, Y.; Chen, Y.; Ji, L. Characterization of soot inside a diesel particulate filter during a nonthermal plasma promoted regeneration step. *Appl. Therm. Eng.* **2019**, *150*, 612–619. [[CrossRef](#)]
85. Fino, D.; Specchia, V. Open issues in oxidative catalysis for diesel particulate abatement. *Powder Technol.* **2008**, *180*, 64–73. [[CrossRef](#)]
86. Mat, S.C.; Idroas, M.Y.; Hamid, M.F.; Zainal, Z.A. Performance and emissions of straight vegetable oils and its blends as a fuel in diesel engine: A review. *Renew. Sustain. Energy Rev.* **2018**, *82*, 808–823. [[CrossRef](#)]
87. Tsuneyoshi, K.; Yamamoto, K. A study on the cell structure and the performances of wall-flow diesel particulate filter. *Energy* **2012**, *48*, 492–499. [[CrossRef](#)]
88. Fino, D.; Bensaïd, S.; Piumetti, M.; Russo, N. A review on the catalytic combustion of soot in Diesel particulate filters for automotive applications: From powder catalysts to structured reactors. *Appl. Catal. A Gen.* **2016**, *509*, 75–96. [[CrossRef](#)]
89. Vander Wal, R.L.; Yezerets, A.; Currier, N.W.; Kim, D.H.; Wang, C.M. HRTEM Study of diesel soot collected from diesel particulate filters. *Carbon* **2007**, *45*, 70–77. [[CrossRef](#)]
90. Lee, J.; Lee, M.W.; Kim, M.J.; Lee, J.H.; Lee, E.J.; Jung, C.; Choung, J.W.; Kim, C.H.; Lee, K.Y. Effects of La incorporation in catalytic activity of Ag/La-CeO₂ catalysts for soot oxidation. *J. Hazard. Mater.* **2021**, *414*, 125523. [[CrossRef](#)]
91. Fang, J.; Zhang, Q.; Meng, Z.; Luo, Y.; Ou, J.; Du, Y.; Zhang, Z. Effects of ash composition and ash stack heights on soot deposition and oxidation processes in catalytic diesel particulate filter. *J. Energy Inst.* **2020**, *93*, 1942–1950. [[CrossRef](#)]
92. Kurien, C.; Srivastava, A.K.; Lesbats, S. Experimental and computational study on the microwave energy based regeneration in diesel particulate filter for exhaust emission control. *J. Energy Inst.* **2020**, *93*, 2133–2147. [[CrossRef](#)]
93. E, J.; Zhao, M.; Zuo, Q.; Zhang, B.; Zhang, Z.; Peng, Q.; Han, D.; Zhao, X.; Deng, Y. Effects analysis on diesel soot continuous regeneration performance of a rotary microwave-assisted regeneration diesel particulate filter. *Fuel* **2020**, *260*, 116353. [[CrossRef](#)]
94. E, J.; Luo, J.; Han, D.; Tan, Y.; Feng, C.; Deng, Y. Effects of different catalysts on light-off temperature of volatile organic components in the rotary diesel particulate filter during the regeneration. *Fuel* **2021**, *310*, 122451.
95. E, J.; Zheng, P.; Han, D.; Zhao, X.; Deng, Y. Effects analysis on soot combustion performance enhancement in a rotary diesel particulate filter unit during continuous microwave heating. *Fuel* **2020**, *276*, 118043. [[CrossRef](#)]

96. E, J.; Zuo, W.; Gao, J.; Peng, Q.; Zhang, Z.; Hieu, P.M. Effect analysis on pressure drop of the continuous regeneration-diesel particulate filter based on NO₂ assisted regeneration. *Appl. Therm. Eng.* **2016**, *100*, 356–366. [[CrossRef](#)]
97. Guo, Y.; Horchler, E.J.; Fairley, N.; Stevanovic, S.; Shang, J.; Ristovski, Z. An experimental investigation of diesel soot thermal-induced oxidation based on the chemical structure evolution. *Carbon* **2022**, *188*, 246–253. [[CrossRef](#)]
98. Huang, T.; Hu, G.; Meng, Z.; Zeng, D. Exhaust temperature control for safe and efficient thermal regeneration of diesel particulate filter. *Appl. Therm. Eng.* **2021**, *189*, 116747. [[CrossRef](#)]
99. Farhan, S.M.; Wang, P.; Wu, Y.; Wu, G.; Lei, L. Evaluation of composition and carbon atoms distribution of the exhaust hydrocarbons by varying post-injection parameters in DI diesel engine. *Fuel* **2021**, *306*, 121662. [[CrossRef](#)]
100. Lisi, L.; Landi, G.; Di Sarli, V. The Issue of Soot-Catalyst Contact in Regeneration of Catalytic Diesel Particulate Filters: A Critical Review. *Catalysts* **2020**, *10*, 1307. [[CrossRef](#)]
101. Tong, Y.; Tan, J.; Meng, Z.; Chen, Z.; Tan, L. Experimental Investigation on the DPF High-Temperature Filtration Performance under Different Particle Loadings and Particle Deposition Distributions. *Processes* **2021**, *9*, 1465. [[CrossRef](#)]
102. Chen, T.; Wu, Z.; Gong, J.; E, J. Numerical Simulation of Diesel Particulate Filter Regeneration Considering Ash Deposit. *Flow Turbul. Combust.* **2016**, *97*, 849–864. [[CrossRef](#)]
103. Meng, Z.; Zhang, J.; Chen, C.; Yan, Y. A numerical investigation of the diesel particle filter regeneration process under temperature pulse conditions. *Heat Mass Transf.* **2016**, *53*, 1589–1602. [[CrossRef](#)]
104. Chong, H.S.; Aggarwal, S.K.; Lee, K.O.; Yang, S.Y.; Seong, H. Experimental Investigation on the Oxidation Characteristics of Diesel Particulates Relevant to DPF Regeneration. *Combust. Sci. Technol.* **2013**, *185*, 95–121. [[CrossRef](#)]
105. R'Mili, B.; Boreave, A.; Meme, A.; Vernoux, P.; Leblanc, M.; Noel, L.; Raux, S.; D'Anna, B. Physico-Chemical Characterization of Fine and Ultrafine Particles Emitted during Diesel Particulate Filter Active Regeneration of Euro5 Diesel Vehicles. *Environ. Sci Technol.* **2018**, *52*, 3312–3319. [[CrossRef](#)]
106. Ruehl, C.; Smith, J.D.; Ma, Y.; Shields, J.E.; Burnitzki, M.; Sobieralski, W.; Ianni, R.; Chernich, D.J.; Chang, M.O.; Collins, J.F.; et al. Emissions during and Real-world Frequency of Heavy-duty Diesel Particulate Filter Regeneration. *Environ. Sci Technol.* **2018**, *52*, 5868–5874. [[CrossRef](#)]
107. Tighe, C.J.; Twigg, M.V.; Hayhurst, A.N.; Dennis, J.S. The kinetics of oxidation of Diesel soots and a carbon black (Printex U) by O₂ with reference to changes in both size and internal structure of the spherules during burnout. *Carbon* **2016**, *107*, 20–35. [[CrossRef](#)]
108. Zhang, Z.; E, J.; Chen, J.; Zhao, X.; Zhang, B.; Deng, Y.; Peng, Q.; Yin, Z. Effects of boiling heat transfer on the performance enhancement of a medium speed diesel engine fueled with diesel and rapeseed methyl ester. *Appl. Therm. Eng.* **2020**, *169*, 114984. [[CrossRef](#)]
109. Harris, S.J.; Maricq, M.M. The role of fragmentation in defining the signature size distribution of diesel soot. *J. Aerosol Sci.* **2002**, *6*, 935–942. [[CrossRef](#)]
110. Beatrice, C.; Iorio, S.D.; Guido, C.; Napolitano, P. Detailed characterization of particulate emissions of an automotive catalyzed DPF using actual regeneration strategies. *Exp. Therm. Fluid Sci.* **2012**, *39*, 45–53. [[CrossRef](#)]
111. Deng, Y.; Cui, J.; E, J.; Zhang, B.; Zhao, X.; Zhang, Z.; Han, D. Investigations on the temperature distribution of the diesel particulate filter in the thermal regeneration process and its field synergy analysis. *Appl. Therm. Eng.* **2017**, *123*, 92–102. [[CrossRef](#)]
112. Deng, Y.; Wang, X.; Chen, G.; Wu, H.; Han, Z.; Li, R. Experimental Study on a Diesel Particulate Filter with Reciprocating Flow. *ACS Omega* **2019**, *4*, 17098–17108. [[CrossRef](#)] [[PubMed](#)]
113. Feng, X.; Ge, Y.; Ma, C.; Tan, J.; Yu, L.; Li, J.; Wang, X. Experimental study on the nitrogen dioxide and particulate matter emissions from diesel engine retrofitted with particulate oxidation catalyst. *Sci. Total Environ.* **2014**, *472*, 56–62. [[CrossRef](#)] [[PubMed](#)]
114. Kuwahara, T.; Nishii, S.; Kuroki, T.; Okubo, M. Complete regeneration characteristics of diesel particulate filter using ozone injection. *Appl. Energy* **2013**, *111*, 652–656. [[CrossRef](#)]
115. Pu, X.; Cai, Y.; Shi, Y.; Wang, J.; Gu, L.; Tian, J.; Fan, R. Carbon Deposit Incineration during Engine Flameout Using Non-Thermal Plasma Injection. *Int. J. Automot. Technol.* **2018**, *19*, 421–432. [[CrossRef](#)]
116. Lee, D.H.; Kim, H.; Song, Y.-H.; Kim, K.-T. Plasma Burner for Active Regeneration of Diesel Particulate Filter. *Plasma Chem. Plasma Process.* **2013**, *34*, 159–173. [[CrossRef](#)]
117. Yao, S.; Kodama, S.; Yamamoto, S.; Fushimi, C.; Madokoro, K.; Mine, C.; Fujioka, Y. Characterization of an uneven DBD reactor for diesel PM removal. *Asia-Pac. J. Chem. Eng.* **2009**, *5*, 701–707. [[CrossRef](#)]
118. Reiter, M.S.; Kockelman, K.M. The problem of cold starts: A closer look at mobile source emissions levels. *Transp. Res. Part D Transp. Environ.* **2016**, *43*, 123–132. [[CrossRef](#)]
119. Gao, J.; Tian, G.; Sornioti, A. On the emission reduction through the application of an electrically heated catalyst to a diesel vehicle. *Energy Sci. Eng.* **2019**, *7*, 2383–2397. [[CrossRef](#)]
120. E, J.; Liu, M.; Deng, Y.; Zhu, H.; Gong, J. Influence analysis of monolith structure on regeneration temperature in the process of microwave regeneration in the diesel particulate filter. *Can. J. Chem. Eng.* **2016**, *94*, 168–174. [[CrossRef](#)]
121. E, J.; Zhao, X.; Xie, L.; Zhang, B.; Chen, J.; Zuo, Q.; Han, D.; Hu, W.; Zhang, Z. Performance enhancement of microwave assisted regeneration in a wall-flow diesel particulate filter based on field synergy theory. *Energy* **2019**, *169*, 719–729.
122. Pallavkar, S.; Kim, T.H.; Rutman, D.; Lin, J.; Ho, T. Active Regeneration of Diesel Particulate Filter Employing Microwave Heating. *Ind. Eng. Chem. Res.* **2008**, *48*, 69–79. [[CrossRef](#)]
123. Palma, V.; Ciambelli, P.; Meloni, E.; Sin, A. Catalytic DPF microwave assisted active regeneration. *Fuel* **2015**, *140*, 50–61. [[CrossRef](#)]

124. Chen, C.; Yao, A.; Yao, C.; Qu, G. Experimental study of the active and passive regeneration procedures of a diesel particulate filter in a diesel methanol dual fuel engine. *Fuel* **2020**, *264*, 116801. [[CrossRef](#)]
125. Chen, H.; Su, X.; Wang, X.; Sun, F.; Zhang, P.; Geng, L.; Wang, H. Filtration Efficiency and Regeneration Behavior in a Catalytic Diesel Particulate Filter with the Use of Diesel/Polyoxymethylene Dimethyl Ether Mixture. *Catalysts* **2021**, *11*, 1425. [[CrossRef](#)]
126. Mishra, A.; Prasad, R. Preparation and Application of Perovskite Catalysts for Diesel Soot Emissions Control: An Overview. *Catal. Rev.* **2014**, *56*, 57–81. [[CrossRef](#)]
127. Caroca, J.; Villata, G.; Fino, D.; Russo, N. Comparison of Different Diesel Particulate Filters. *Top. Catal.* **2009**, *52*, 2076–2082. [[CrossRef](#)]
128. Du, Y.; Wen, B.; Shu, R.; Cao, L.; Wang, W. Potassium titanate whiskers on the walls of cordierite honeycomb ceramics for soot catalytic combustion. *Ceram. Int.* **2021**, *47*, 34828–34835. [[CrossRef](#)]
129. Du, Y.; Meng, Z.; Fang, J.; Qin, Y.; Jiang, Y.; Li, S.; Li, J.; Chen, C.; Bai, W. Characterization of soot deposition and oxidation process on catalytic diesel particulate filter with ash loading through an optimized visualized method. *Fuel* **2019**, *243*, 251–261. [[CrossRef](#)]
130. Colombo, C.; Monhemius, A.J.; Plant, J.A. Platinum, palladium and rhodium release from vehicle exhaust catalysts and road dust exposed to simulated lung fluids. *Ecotoxicol. Environ. Saf.* **2008**, *71*, 722–730. [[CrossRef](#)]
131. Zhang, Z.; Ye, J.; Lv, J.; Xu, W.; Tan, D.; Jiang, F.; Huang, H. Investigation on the effects of non-uniform porosity catalyst on SCR characteristic based on the field synergy analysis. *J. Environ. Chem. Eng.* **2022**, *10*, 107056. [[CrossRef](#)]
132. Kong, H.; Yamamoto, K. Simulation on soot deposition in in-wall and on-wall catalyzed diesel particulate filters. *Catal. Today* **2019**, *332*, 89–93. [[CrossRef](#)]
133. Liu, S.; Wu, X.; Weng, D.; Li, M.; Ran, R. Roles of Acid Sites on Pt/H-ZSM5 Catalyst in Catalytic Oxidation of Diesel soot. *ACS Catal.* **2015**, *5*, 909–919. [[CrossRef](#)]
134. Oh, D.-K.; Lee, Y.-J.; Lee, K.-Y.; Park, J.-S. Nitrogen Monoxide and Soot Oxidation in Diesel Emissions with Platinum–Tungsten/Titanium Dioxide Catalysts: Tungsten Loading Effect. *Catalysts* **2020**, *10*, 1283. [[CrossRef](#)]
135. E, J.; Zhao, X.; Liu, G.; Zhang, B.; Zuo, Q.; Wei, K.; Li, H.; Han, D.; Gong, J. Effects analysis on optimal microwave energy consumption in the heating process of composite regeneration for the diesel particulate filter. *Appl. Energy* **2019**, *254*, 113736. [[CrossRef](#)]
136. Palma, V.; Russo, P.; Matarazzo, G.; Ciambelli, P. Microwave improvement of catalyst performance in soot oxidation without additives. *Appl. Catal. B Environ.* **2007**, *70*, 254–260. [[CrossRef](#)]
137. Bayat, M.; Hamidi, M.; Dehghani, Z.; Rahimpour, M.R. Sorption-enhanced Fischer–Tropsch synthesis with continuous adsorbent regeneration in GTL technology: Modeling and optimization. *J. Ind. Eng. Chem.* **2014**, *20*, 858–869. [[CrossRef](#)]
138. Bogdanić, M.; Behrendt, F.; Mertins, F. The influence of a 2-component model on the computed regeneration behaviour of an uncoated diesel particulate filter. *Chem. Eng. Sci.* **2008**, *63*, 2601–2613. [[CrossRef](#)]
139. Torregrosa, A.J.; Serrano, J.R.; Arnau, F.J.; Piqueras, P. A fluid dynamic model for unsteady compressible flow in wall-flow diesel particulate filters. *Energy* **2011**, *36*, 671–684. [[CrossRef](#)]
140. Müller, J.-O.; Frank, B.; Jentoft, R.E.; Schlögl, R.; Su, D.S. The oxidation of soot particulate in the presence of NO₂. *Catal. Today* **2012**, *191*, 106–111. [[CrossRef](#)]
141. Azambre, B.; Collura, S.; Darcy, P.; Trichard, J.M.; Da Costa, P.; García-García, A.; Bueno-López, A. Effects of a Pt/Ce_{0.68}Zr_{0.32}O₂ catalyst and NO₂ on the kinetics of diesel soot oxidation from thermogravimetric analyses. *Fuel Process. Technol.* **2011**, *92*, 363–371. [[CrossRef](#)]
142. Tighe, C.J.; Twigg, M.V.; Hayhurst, A.N.; Dennis, J.S. The kinetics of oxidation of Diesel soots by NO₂. *Combust. Flame* **2012**, *159*, 77–90. [[CrossRef](#)]
143. Serrano, J.R.; Arnau, F.J.; Piqueras, P.; García-Afonso, Ó. Packed bed of spherical particles approach for pressure drop prediction in wall-flow DPFs (diesel particulate filters) under soot loading conditions. *Energy* **2013**, *58*, 644–654. [[CrossRef](#)]
144. Schejbal, M.; Štěpánek, J.; Marek, M.; Kočí, P.; Kubíček, M. Modelling of soot oxidation by NO₂ in various types of diesel particulate filters. *Fuel* **2010**, *89*, 2365–2375. [[CrossRef](#)]
145. Millo, F.; Andreatta, M.; Rafigh, M.; Mercuri, D.; Pozzi, C. Impact on vehicle fuel economy of the soot loading on diesel particulate filters made of different substrate materials. *Energy* **2015**, *86*, 19–30. [[CrossRef](#)]
146. Tsuneyoshi, K.; Yamamoto, K. Experimental study of hexagonal and square diesel particulate filters under controlled and uncontrolled catalyzed regeneration. *Energy* **2013**, *60*, 325–332. [[CrossRef](#)]
147. Zhang, Z.; Tian, J.; Li, J.; Cao, C.; Wang, S.; Lv, J.; Zheng, W.; Tan, D. The development of diesel oxidation catalysts and the effect of sulfur dioxide on catalysts of metal-based diesel oxidation catalysts: A review. *Fuel Process. Technol.* **2022**, *234*, 107317. [[CrossRef](#)]
148. Stepień, Z.; Ziemiański, L.; Żak, G.; Wojtasik, M.; Jęczmionek, Ł.; Burnus, Z. The evaluation of fuel borne catalyst (FBC's) for DPF regeneration. *Fuel* **2015**, *161*, 278–286. [[CrossRef](#)]
149. Xiao, G.; Li, B.; Tian, H.; Leng, X.; Long, W. Numerical study on flow and pressure drop characteristics of a novel type asymmetric wall-flow diesel particulate filter. *Fuel* **2020**, *267*, 117148. [[CrossRef](#)]
150. Yang, J.; Stewart, M.; Maupin, G.; Herling, D.; Zelenyuk, A. Single wall diesel particulate filter (DPF) filtration efficiency studies using laboratory generated particles. *Chem. Eng. Sci.* **2009**, *64*, 1625–1634. [[CrossRef](#)]
151. Liati, A.; Eggenschwiler, P.D. Characterization of particulate matter deposited in diesel particulate filters: Visual and analytical approach in macro-, micro- and nano-scales. *Combust. Flame* **2010**, *157*, 1658–1670. [[CrossRef](#)]

152. Swanson, J.; Watts, W.; Kittelson, D.; Newman, R.; Ziebarth, R. Filtration Efficiency and Pressure Drop of Miniature Diesel Particulate Filters. *Aerosol Sci. Technol.* **2013**, *47*, 452–461. [[CrossRef](#)]
153. Liu, Y.; Gong, J.; Fu, J.; Cai, H.; Long, G. Nanoparticle motion trajectories and deposition in an inlet channel of wall-flow diesel particulate filter. *J. Aerosol Sci.* **2009**, *40*, 307–323. [[CrossRef](#)]
154. Sappok, A.; Wang, Y.; Wang, R.-Q.; Kamp, C.; Wong, V. Theoretical and Experimental Analysis of Ash Accumulation and Mobility in Ceramic Exhaust Particulate Filters and Potential for Improved Ash Management. *SAE Int. J. Fuels Lubr.* **2014**, *7*, 511–524. [[CrossRef](#)]
155. Hamaker, H.C. The London—Van der Waals attraction between spherical particles. *Physica* **1937**, *4*, 1058–1072. [[CrossRef](#)]
156. Wang, Y.; Kamp, C.J.; Wang, Y.; Toops, T.J.; Su, C.; Wang, R.; Gong, J.; Wong, V.W. The origin, transport, and evolution of ash in engine particulate filters. *Appl. Energy* **2020**, *263*, 114631. [[CrossRef](#)]
157. Liu, Y.Q.; Keane, M.; Ensell, M.; Miller, W.; Kashon, M.; Ong, T.M.; Mauderly, J.; Lawson, D.; Gautam, M.; Zielinska, B.; et al. In vitro genotoxicity of exhaust emissions of diesel and gasoline engine vehicles operated on a unified driving cycle. *J. Environ. Monit.* **2005**, *7*, 60–66. [[CrossRef](#)]
158. Pu, Y.H.; Reddy, J.K.; Samuel, S. Machine learning for nano-scale particulate matter distribution from gasoline direct injection engine. *Appl. Therm. Eng.* **2017**, *125*, 336–345. [[CrossRef](#)]
159. Luo, Y.; Zhu, L.; Fang, J.; Zhuang, Z.; Guan, C.; Xia, C.; Xie, X.; Huang, Z. Size distribution, chemical composition and oxidation reactivity of particulate matter from gasoline direct injection (GDI) engine fueled with ethanol-gasoline fuel. *Appl. Therm. Eng.* **2015**, *89*, 647–655. [[CrossRef](#)]
160. Awad, O.I.; Ma, X.; Kamil, M.; Ali, O.M.; Zhang, Z.; Shuai, S. Particulate emissions from gasoline direct injection engines: A review of how current emission regulations are being met by automobile manufacturers. *Sci. Total Environ.* **2020**, *718*, 137302. [[CrossRef](#)]
161. Raza, M.; Chen, L.; Leach, F.; Ding, S. A Review of Particulate Number (PN) Emissions from Gasoline Direct Injection (GDI) Engines and Their Control Techniques. *Energies* **2018**, *11*, 1417. [[CrossRef](#)]
162. Wang, C.; Xu, H.; Herreros, J.M.; Wang, J.; Cracknell, R. Impact of fuel and injection system on particle emissions from a GDI engine. *Appl. Energy* **2014**, *132*, 178–191. [[CrossRef](#)]
163. Hoseinpour, M.; Sadrnia, H.; Ghobadian, B.; Tabasizadeh, M. Effects of gasoline fumigation on exhaust emission and performance characteristics of a diesel engine with mechanically-controlled fuel injection pump. *Environ. Prog. Sustain. Energy* **2018**, *37*, 1845–1852. [[CrossRef](#)]
164. Jang, J.; Lee, J.; Choi, Y.; Park, S. Reduction of particle emissions from gasoline vehicles with direct fuel injection systems using a gasoline particulate filter. *Sci. Total Environ.* **2018**, *644*, 1418–1428. [[CrossRef](#)] [[PubMed](#)]
165. Jiang, C.; Li, Z.; Qian, Y.; Wang, X.; Zhang, Y.; Lu, X. Influences of fuel injection strategies on combustion performance and regular/irregular emissions in a turbocharged gasoline direct injection engine: Commercial gasoline versus multi-components gasoline surrogates. *Energy* **2018**, *157*, 173–187. [[CrossRef](#)]
166. Mamakos, A.; Steining, N.; Martini, G.; Dilara, P.; Drossinos, Y. Cost effectiveness of particulate filter installation on Direct Injection Gasoline vehicles. *Atmos. Environ.* **2013**, *77*, 16–23. [[CrossRef](#)]
167. Yu, S.; Yin, B.; Bi, Q.; Jia, H.; Chen, C. Effects of gasoline and ethanol on inner flows and swallowtail-like spray behaviors of elliptical GDI injector. *Fuel* **2021**, *294*, 120543. [[CrossRef](#)]
168. Montanaro, A.; Allocca, L. Study of Liquid and Vapor Phases of a GDI Spray. *Combust. Sci. Technol.* **2019**, *191*, 1600–1608. [[CrossRef](#)]
169. Yang, J.; Roth, P.; Durbin, T.D.; Johnson, K.C.; Cocker, D.R., 3rd; Asa-Awuku, A.; Brezny, R.; Geller, M.; Karavalakis, G. Gasoline Particulate Filters as an Effective Tool to Reduce Particulate and Polycyclic Aromatic Hydrocarbon Emissions from Gasoline Direct Injection (GDI) Vehicles: A Case Study with Two GDI Vehicles. *Environ. Sci. Technol.* **2018**, *52*, 3275–3284. [[CrossRef](#)]
170. Mu, M.; Li, X.; Qiu, Y.; Shi, Y. Study on a New Gasoline Particulate Filter Structure Based on the Nested Cylinder and Diversion Channel Plug. *Energies* **2019**, *12*, 2045. [[CrossRef](#)]
171. Arunachalam, H.; Pozzato, G.; Hoffman, M.A.; Onori, S. Modeling the thermal and soot oxidation dynamics inside a ceria-coated gasoline particulate filter. *Control Eng. Pract.* **2020**, *94*, 104199. [[CrossRef](#)]
172. Boger, T.; Rose, D.; Nicolin, P.; Gunasekaran, N.; Glasson, T. Oxidation of Soot (Printex[®] U) in Particulate Filters Operated on Gasoline Engines. *Emiss. Control Sci. Technol.* **2015**, *1*, 49–63. [[CrossRef](#)]
173. Yamamoto, K.; Kondo, S.; Suzuki, K. Filtration and regeneration performances of SiC fiber potentially applied to gasoline particulates. *Fuel* **2019**, *243*, 28–33. [[CrossRef](#)]
174. Myung, C.-L.; Kim, J.; Jang, W.; Jin, D.; Park, S.; Lee, J. Nanoparticle Filtration Characteristics of Advanced Metal Foam Media for a Spark Ignition Direct Injection Engine in Steady Engine Operating Conditions and Vehicle Test Modes. *Energies* **2015**, *8*, 1865–1881. [[CrossRef](#)]
175. Mu, M.; Sjöblom, J.; Sharma, N.; Ström, H.; Li, X. Experimental Study on the Flow Field of Particles Deposited on a Gasoline Particulate Filter. *Energies* **2019**, *12*, 2701. [[CrossRef](#)]
176. Zuo, Q.; Zhu, X.; Zhang, J.; Zhang, B.; Tang, Y.; Xie, Y.; Zhang, X.; Zhu, G.; Wang, Z. Effects of exhaust parameters on temperature and pressure drop of the gasoline particulate filter in the regeneration equilibrium state. *Fuel* **2019**, *257*, 116019. [[CrossRef](#)]
177. Kim, M.J.; Lee, E.J.; Lee, E.; Kim, D.H.; Lee, D.-W.; Kim, C.H.; Lee, K.-Y. Ag-doped manganese oxide catalyst for gasoline particulate filters: Effect of crystal phase on soot oxidation activity. *Appl. Surf. Sci.* **2021**, *569*, 151041. [[CrossRef](#)]

178. Liu, J.; Ulishney, C.; Dumitrescu, C.E. Effect of spark timing on the combustion stages seen in a heavy-duty compression-ignition engine retrofitted to natural gas spark-ignition operation. *SAE Int. J. Engines* **2021**, *14*, 335–344. [[CrossRef](#)]
179. Hu, L.; Tian, Q.; Zou, C.; Huang, J.; Ye, Y.; Wu, X. A study on energy distribution strategy of electric vehicle hybrid energy storage system considering driving style based on real urban driving data. *Renew. Sustain. Energy Rev.* **2022**, *162*, 112416. [[CrossRef](#)]
180. Hu, L.; Ou, J.; Huang, J.; Wang, F.; Wang, Y.; Ren, B.; Peng, H.; Zhou, L. Safety Evaluation of Pedestrian-Vehicle Interaction at Signalized Intersections in Changsha, China. *J. Trans. Saf. Secur.* **2021**. [[CrossRef](#)]
181. Ma, Y.; Liu, C.; E, J.; Mao, X.; Yu, Z. Research on modeling and parameter sensitivity of flow and heat transfer process in typical rectangular microchannels: From a data-driven perspective. *Int. J. Therm. Sci.* **2022**, *172*, 107356. [[CrossRef](#)]
182. Tan, Y.; E, J.; Chen, J.; Liao, G.; Zhang, F.; Li, J. Investigation on combustion characteristics and thermal performance of a three rearward-step structure micro combustor fueled by premixed hydrogen/air. *Renew. Energy* **2022**, *186*, 486–504. [[CrossRef](#)]
183. Zuo, H.; Zhang, B.; Huang, Z.; Wei, K.; Tan, J. Effect analysis on SOC values of the power lithium manganese battery during discharging process and its intelligent estimation. *Energy* **2022**, *238*, 121854. [[CrossRef](#)]
184. Zuo, H.; Tan, J.; Wei, K.; Huang, Z.; Zhong, D.; Xie, F. Effects of different poses and wind speeds on wind-induced vibration characteristics of a dish solar concentrator system. *Renew. Energy* **2021**, *168*, 1308–1326. [[CrossRef](#)]
185. Zuo, H.; Liu, G.; E, J.; Zuo, W.; Wei, K.; Hu, W.; Tan, J.; Zhong, D. Catastrophic analysis on the stability of a large dish solar thermal power generation system with wind-induced vibration. *Sol. Energy* **2019**, *183*, 40–49. [[CrossRef](#)]
186. Han, D.; E, J.; Deng, Y.; Zhao, X.; Feng, C.; Chen, J.; Leng, E.; Liao, G.; Zhang, F. A review of studies using hydrocarbon reduction measures for reducing hydrocarbon emissions from cold start of gasoline engine. *Renew. Sustain. Energy Rev.* **2021**, *135*, 110079. [[CrossRef](#)]
187. Chen, L.; Deng, Y.; Feng, C.; Han, W.; E, J.; Wang, C.; Han, D.; Zhang, B. Effects of zeolite molecular sieve on the hydrocarbon adsorbent performance of gasoline engine of during cold start. *Fuel* **2022**, *310*, 122427. [[CrossRef](#)]
188. Feng, C.; Deng, Y.; Tan, Y.; Han, W.; E, J.; Chen, L.; Han, D. Experimental and simulation study on the effect of ZSM-5 hydrocarbon catcher on the emission of gasoline engine during cold start. *Fuel* **2022**, *313*, 122661. [[CrossRef](#)]
189. Li, Y.; Tang, W.; Chen, Y.; Liu, J.; Lee, C.F. Potential of acetone-butanol-ethanol (ABE) as a biofuel. *Fuel* **2019**, *242*, 673–686. [[CrossRef](#)]
190. Li, Y.; Meng, L.; Nithyanandan, K.; Lee, T.H.; Lin, Y.; Lee, C.F.; Liao, S. Combustion, performance and emissions characteristics of a spark-ignition engine fueled with isopropanol-n-butanol-ethanol and gasoline blends. *Fuel* **2016**, *184*, 864–872. [[CrossRef](#)]